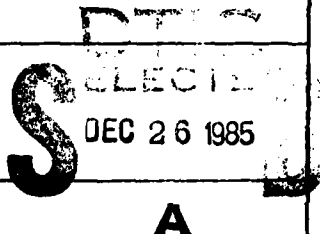


AD-A162 753

DTIC  
S \* D  
REL. IN E  
DEC 26 1985  
A

UNCLASSIFIED

SECURITY CLASSIFICATION OF THIS PAGE (When Data Entered)

REPORT DOCUMENTATION PAGE		READ INSTRUCTIONS BEFORE COMPLETING FORM
1. REPORT NUMBER	2. GOVT ACCESSION NO.	3. RECIPIENT'S CATALOG NUMBER
	AD-A162 753	
4. TITLE (and Subtitle)	5. TYPE OF REPORT & PERIOD COVERED	
An Evaluation of the Properties of Ferromagnetic Liquids at Millimeter Wave Frequencies	2nd Annual Report 21 Dec 82-30 Oct 85	
	6. PERFORMING ORG. REPORT NUMBER	
7. AUTHOR(s)	8. CONTRACT OR GRANT NUMBER(s)	
Dr. J. Popplewell Dr J P Llewellyn and Mr P Davies	DAJA 45-83-C-0026 R&D 4130-MS-01	
9. PERFORMING ORGANIZATION NAME AND ADDRESS	10. PROGRAM ELEMENT, PROJECT, TASK AREA & WORK UNIT NUMBERS	
University College of North Wales Department of Physics Bangor, Gwynedd LL57 2UW	61002ALL161102BH5704	
11. CONTROLLING OFFICE NAME AND ADDRESS	12. REPORT DATE	
US ARMY RESEARCH DEVELOPMENT AND STANDARDIZATION GROUP-UK P.O. Box 65, FPO NY, 09510	October 1985	
	13. NUMBER OF PAGES	
	76	
14. MONITORING AGENCY NAME & ADDRESS (if different from Controlling Office)	15. SECURITY CLASS. (of this report)	
U.S. Army Research Office P.O. Box 12211 Research Triangle Park, NC 27709	UNCLASSIFIED	
	15a. DECLASSIFICATION/DOWNGRADING SCHEDULE	
16. DISTRIBUTION STATEMENT (of this Report)		
Approved for public release, distribution unlimited		
17. DISTRIBUTION STATEMENT (of the abstract entered in Block 20, if different from Report)		
<div style="text-align: right;">  </div>		
18. SUPPLEMENTARY NOTES		
<div style="text-align: center;">  </div>		
19. KEY WORDS (Continue on reverse side if necessary and identify by block number)		
Magnetic Fluids, Composites, Thin Films, Microwave, Dichroism, Birefringence		
20. ABSTRACT (Continue on reverse side if necessary and identify by block number)		
<p>Ferrofluid composites containing polystyrene, tin, copper, aluminium, carbon and silver particles 1 to 50 <math>\mu\text{m}</math> in diameter have been prepared by dispersing the particles in ferrofluids with <math>M_s = 400</math> to 800 G. Thin film samples 1 <math>\mu\text{m}</math> to 1 mm thick have been studied using a 3 mm microwave source and Fourier Transform Spectrometry. Large microwave absorptions (60%) which are induced by small fields of less than 100 Oe have been observed in thin film composites containing</p>		

DD FORM 1 JAN 73 1473 EDITION OF 7 NOV 65 IS OBSOLETE

UNCLASSIFIED

SECURITY CLASSIFICATION OF THIS PAGE (When Data Entered)

metal particles. Magnetic absorptions arise from chain formation in the composite and this has been modelled using Monte-Carlo simulations. Good agreement between the observations and theoretical predictions is obtained.

*Keywords include:*

19

Accession For	
NTIS CRA&I	<input checked="" type="checkbox"/>
DTIC TAB	<input type="checkbox"/>
Unannounced	<input type="checkbox"/>
Justification	
By	
Distribution	
Availability Codes	
Avail and/or Special	
At	AI

1  
2  
3  
4  
5  
6  
7  
8  
9  
10  
11  
12  
13  
14  
15  
16  
17  
18  
19  
20  
21  
22  
23  
24  
25  
26  
27  
28  
29  
30  
31  
32  
33  
34  
35  
36  
37  
38  
39  
40  
41  
42  
43  
44  
45  
46  
47  
48  
49  
50  
51  
52  
53  
54  
55  
56  
57  
58  
59  
60  
61  
62  
63  
64  
65  
66  
67  
68  
69  
70  
71  
72  
73  
74  
75  
76  
77  
78  
79  
80  
81  
82  
83  
84  
85  
86  
87  
88  
89  
90  
91  
92  
93  
94  
95  
96  
97  
98  
99  
00

<u>List of Contents</u>	<u>Page</u>
List of Captions	(iii)
List of Symbols	(vi)
Abstract	
1 Introduction	
1.1 Ferrofluid Composites	1
1.2 Microwave Properties of Ferrofluid Composites	2
2 Magnetic and Optical Properties of Ferrofluids	4
2.1 Magnetic Properties	4
2.1 (a) Modes of Magnetisation and Superparamagnetism	5
2.1 (b) The Magnetisation Curve	8
2.2 Optical Properties of Magnetic Fluids	9
3 Magnetic Properties of Ferrofluid Composites	17
3.1 Composites Containing Polystyrene Spheres	17
3.2 Relaxation Effects in Composite Structures	18
4 Experimental Procedure	21
4.1 Preparation of the Composite Carrier Ferrofluids Containing Magnetite Particles	21
4.2 Preparation of Ferrofluid Composites	23
4.2 (a) Preparation of Samples Containing Polystyrene Spheres for Optical Studies	23
4.2 (b) Preparation of Samples Containing Non- Magnetic Metallic Particles for Optical Studies	25
4.2 (c) Preparation of Samples for Microwave Measurements	25
4.2 (d) Preparation of Microwave Samples Using Z-Cut Crystalline Quartz Plates	26
4.3 Microwave Experiments	27
4.3 (a) Single Wavelength ( $\lambda = 3 \text{ mm}$ ) Experiments	27
4.3 (b) Fourier Transform Spectroscopy (FTS)	31

4.4 Monte-Carlo Simulations	36
4.4 (a) The Spatial Distribution Function	38
5 Results	
5.1 Magnetically Induced Microwave Absorption Effects	39
5.1 (a) Single Frequency Source	39
5.1 (b) Fourier Transform Spectroscopy	44
5.1 (c) Relaxation Measurements	46
5.2 Monte-Carlo Simulations	51
5.2 (a) Theoretical Configurations of a Composite Containing 1 $\mu\text{m}$ diameter Polystyrene Spheres	51
5.2 (b) Spatial Distribution Function $g(r,\theta)$	51
5.2 (c) Energy Considerations	54
6 Recommendations and Future Work	60
Acknowledgements	63
References	64
Publications	66

List of Figures

<u>Figure</u>	<u>Caption</u>	<u>Page</u>
1	Room Temperature Magnetisation Curve of a 60 A Cobalt Ferrofluid	6
2	Low Temperature Magnetisation Curve of a 60 A Cobalt Ferrofluid	7
3 (i)	Decay of Magnetisation with Time	12
(ii)	Decay of Birefringence with Time	12
4	Wavelength Dependence of Optical Dichroism and Birefringence	14
5	Interacting Polystyrene Spheres, H Parallel to Film	19
6	Interacting Polystyrene Spheres, H Perpendicular to Film	19
7	Reaction Mechanism of the Production of 100 A Magnetite Particles	22
8	Schematic Diagram of Surfactant Coating of Magnetite Particles	22
9	Composite Colloid Sample	24
10	TPX Cell for Microwave Measurements	24
11	3 mm Wavelength Microwave Apparatus	28
12	Different Field Orientations for the Measurement of $I_0$ and I	30
13	Apparatus for Measuring Dichroism and Birefringence at Millimetre Wavelengths	31
14	The Fourier Transform Spectrometer	34
15	An Amplitude Modulated Interferogram	35

<u>Figure</u>	<u>Caption</u>	<u>Page</u>
16	Plot of Transmission versus Field for Tin Particles	40
17	Plot of Final Transmission, $T_f$ versus Concentration for Tin Particles	41
18	$T_f$ Versus Concentration for Different Materials	43
19	Plot of $I/I_0$ Versus Wavelength for Aluminium Particles in Decalin Based Ferrofluid	45
20	Composites Colloid Containing Polystyrene Spheres in a Field of $\approx 100$ Oe Parallel to Layer	47
21	Composite Colloid shown in Figure 20 2-3 Seconds after Removal of Field	47
22	Composite Colloid Containing Tin Particles in a Field of About 100 Oe Parallel to Layer	47
23	Composite Structure 2-3 Seconds after Removal of Field	47
24	Relaxation of Tin and Copper Particles	49
25	Relaxation of Aluminium Particles	49
26	Monte-Carlo Configuration with $H$ Parallel to Film, $c = 0.16$	52
27	Monte-Carlo Configuration with $H$ Parallel to Film, $c = 0.06$	52
28	Monte-Carlo Configuration with $H$ Perpendicular to Film, $c = 0.16$	52
29	Composite Colloid Containing Polystyrene Spheres in Field of 20 Oe Applied Parallel to the Film, $c = 0.16$	53

<u>Figure</u>	<u>Caption</u>	<u>Page</u>
30	Composite Colloid Containing Polystyrene Spheres in a field of 20 Oe Applied Parallel to the Film, $c = 0.06$	53
31	Composite Colloid Containing Polystyrene Spheres in a Field of 20 Oe Applied Perpendicularly to the Film; $c = 0.16$	53
32	The Spatial Distribution Function of Figure 26	55
33	The SDF of Figure 27	56
34	The SDF pf Figure 28	57
35	Internal Energy of a Composite Colloid Plotted as a Function of $\theta$ the Angle between the Field and the Plane of the Film	58

List of Symbols

$I_s$	Saturation magnetisation
$\epsilon$	Packing fraction
$\eta$	Viscosity
$I_{eff}$	Effective magnetisation
$k$	Boltzmann's constant
$T$	Absolute temperature
$U$	Magnetostatic energy
$\mu$	Magnetic moment
$r$	Interparticle separation
$a$	Particle radius
$d$	Particle diameter
$V$	Particle volume
$c$	Dimensionless particle concentration
$\Delta n$	Birefringence
$n_0$	Isotropic refractive index
$(g_1 - g_{11})$	Difference in optical polarizabilities
$p$	$\mu H / kT$
$L(p)$	The Langevin Function
$\xi(q)$	Coupling function
$f(y)$	Particle size distribution function
$\Delta k$	Dichroism
$(h_1 - h_{11})$	Imaginary component of the optical polarizabilities
$\sigma$	Standard deviation of $f(y)$
$K$	Anisotropy constant
$X$	Carrier fluid susceptibility
$X_{eff}$	Effective magnetic susceptibility
$N_s$	Demagnetising factor of a sample
$N_p$	" " " " particle
$E$	Interaction dipolar energy

- θ Angle between field and line joining two particles
- Γ Triangular lattice stability parameter
- D Einstein diffusion coefficient
- λ Wavelength

Abstract

Keywords: Magnetic Fluids, Composites, Thin Films, Microwave, Dichroism, Birefringence.

Ferrofluid composites containing polystyrene, tin, copper, aluminium, carbon and silver particles 1 to 50  $\mu\text{m}$  in diameter have been prepared by dispersing the particles in ferrofluids with  $\bar{M}_g = 400$  to 800 G. Thin film samples 1  $\mu\text{m}$  to 1 mm thick have been studied using a 3 mm microwave source and Fourier Transform Spectrometry. Large microwave absorptions (60%) which are induced by small fields of less than 100 Oe have been observed in thin film composites containing metal particles. Magnetic absorptions arise from chain formation in the composite and this has been modelled using Monte-Carlo simulations. Good agreement between the observations and theoretical predictions is obtained.

## 1 INTRODUCTION

Magnetic fluids (ferrofluids) have recently been shown to possess a magnetic dichroism, birefringence and Faraday rotation at microwave wavelengths (Birch et al 1985). These effects are significant and their origin depends on the structure of the magnetic fluids. However, a much larger magnetically induced dichroism is observed in ferrofluid composites. The effect is potentially more exciting and more likely to lead to the development of new devices for use in the millimetre wavelength range.

### 1.1 Ferrofluid Composites

A ferrofluid composite consists of macroscopic non-magnetic particles between  $10^{-4}$  and  $10^{-2}$ cm in diameter dispersed in a ferrofluid carrier. Since the ferrofluid itself is a dispersion of colloidal magnetic particles in a non-magnetic liquid carrier it is important to distinguish between these magnetic particles and the much larger non-magnetic particles which are subsequently added to the ferrofluid to form the composite. Since the colloidal magnetic particles are some 100 times smaller in diameter than the non-magnetic particles of the composite, to a first approximation the larger particles can be considered to be dispersed in a homogeneous magnetic medium, the ferrofluid, which has well defined magnetic properties. If the composite particle size were progressively reduced, however, a situation would develop that is analagous to the formation of an alloy when the magnetic and non-magnetic particle sizes become comparable. It is interesting to speculate how the magnetic properties of the system would change as the composite particle size approaches that of the 'alloy' state. It is conceivable, for example, that the magnetic birefringence, dichroism, etc., would change substantially or even disappear. To resolve this

question studies of the microwave properties of composites are contemplated which include both an experimental investigation and a theoretical analysis using Monte-Carlo simulations.

#### 1.2 Microwave Properties of Ferrofluid Composites

In a magnetic field the non-magnetic particles of the composite acquire a strong induced diamagnetic moment (Section 3) which causes the particles to aggregate into chains which align in the field direction. It is this alignment, when the particles are metallic, which is responsible for the strong magnetic dichroism observed in the microwave region.

The purpose of the work undertaken and reported here has been to study and measure the microwave properties of a number of composites containing particles of different materials, shape and concentration. Such measurements are necessary before the usefulness of ferrofluid composites in devices such as modulators, polarisers or isolators can be ascertained.

In order to measure the absorption, magnetic birefringence and dichroism through a wide wavelength range a Microwave Fourier Transform Spectrometer (FTS) has been constructed. Most measurements so far undertaken have been restricted, however, to measurements at a fixed 3 mm wavelength using an Impatt diode as a microwave source and a Golay pneumatic cell as detector.

Monte-Carlo simulations have also been undertaken to model the particle distribution within the composites and in this way establish by theoretical means the most appropriate structures likely to give a large magnetic birefringence and dichroism. The simulations have been valuable and excellent agreement between the theoretical predictions and experimental observations has been obtained.

It is clear from the studies already undertaken that the ferrofluid composites have extremely important properties in the microwave range. However, other features which arise from the anisotropy induced by an applied magnetic field are also worthy of investigation. In this respect attention should be directed to studies of the magnetic field induced anisotropic electrical conductivity and dielectric constant as well as rheological properties.

## 2 MAGNETIC AND OPTICAL PROPERTIES OF FERROFLUIDS

Most of the work undertaken and discussed in this Report has been concerned with the microwave properties of ferrofluid composites. The properties observed, however, depend on both the nature of the particulate material in the composite and the ferrofluid itself which acts as a carrier for the particles. The ferrofluid magnetisation curve, magnetic strength (saturation magnetisation  $\bar{I}_s$ ) and viscosity are important in determining the behaviour of the composite and therefore any likely application. As a consequence this section of the Report is devoted to a discussion of the properties of the ferrofluid carrier.

### 2.1 Magnetic Properties

Magnetic fluids are prepared by dispersing single domain magnetic particles such as  $\text{Fe}_3\text{O}_4$ , iron, nickel or cobalt in a carrier fluid such as water, a hydrocarbon oil, a diester or toluene. The particles are made small, approximately 100Å in diameter, and are coated with a surfactant to produce colloidal stability in the presence of both magnetostatic and van der Waal's attractive forces.

The strength of the magnetic fluid as represented by its saturation magnetisation  $\bar{I}_s$  is determined by the particle packing fraction  $\epsilon$  and the saturation magnetisation of the particle material  $I_s$ . Thus

$$\bar{I}_s = \epsilon I_s \quad (1)$$

The viscosity  $\eta$  also depends on the particle concentration and for a magnetic fluid containing  $\text{Fe}_3\text{O}_4$  particles with  $\epsilon = 0.02$ ,  $\eta$  is typically 10 cp.

The criteria affecting the stability of the ferrofluid used as the carrier in the preparation of composites can also be applied to the larger non-magnetic particles of the composite. In this case

the particles are at least two orders of magnitude larger than the colloidal magnetic particles of the ferrofluid and even though the effective magnetisation  $I_{eff}$  is smaller the particles of the composite migrate more readily in a field gradient. Thus for colloidal  $Fe_3O_4$  particles with  $a = 50A$ ,  $I_s = 500 \text{ emu/cc}$  and the larger composite particles with  $a = 10^{-4} \text{ cm}$ ,  $I_{eff} = 15 \text{ emu/cc}$  the criteria for stability (Popplewell et al 1985)

$$S = \frac{V\epsilon}{\epsilon} = \frac{4\pi I_s VHa^3}{3kT} \quad (2)$$

$$\text{gives } \frac{S(\text{colloid})}{S(\text{composite})} = 4 \times 10^{-6}$$

Thus by this criterion the colloidal particles are  $\approx 10^6$  times more stable in a field gradient  $\nabla H$  than the composite particles. It follows that though a substantial migration of the composite particles is likely in a field gradient of  $10^2 \text{ Oe/cm}$  the colloidal particles would remain unaffected.

#### 2.1(a) Modes of Magnetisation and Superparamagnetism

The room temperature magnetisation curve for a ferrofluid containing 60 A radius cobalt particles dispersed in a diester carrier is shown in Figure 1. The curve is similar to that expected for a paramagnetic gas with the magnetic moment equal to that of a cobalt particle, radius 60 A. This superparamagnetic state has no remanence or coercivity. The magnetisation curve of the ferrofluid below its melting point is, however, different and an appreciable remanence and coercivity are observed (Figure 2). For a system containing relatively large particles,  $a \approx 60A$ , superparamagnetism is only observed in the liquid state. A system containing smaller

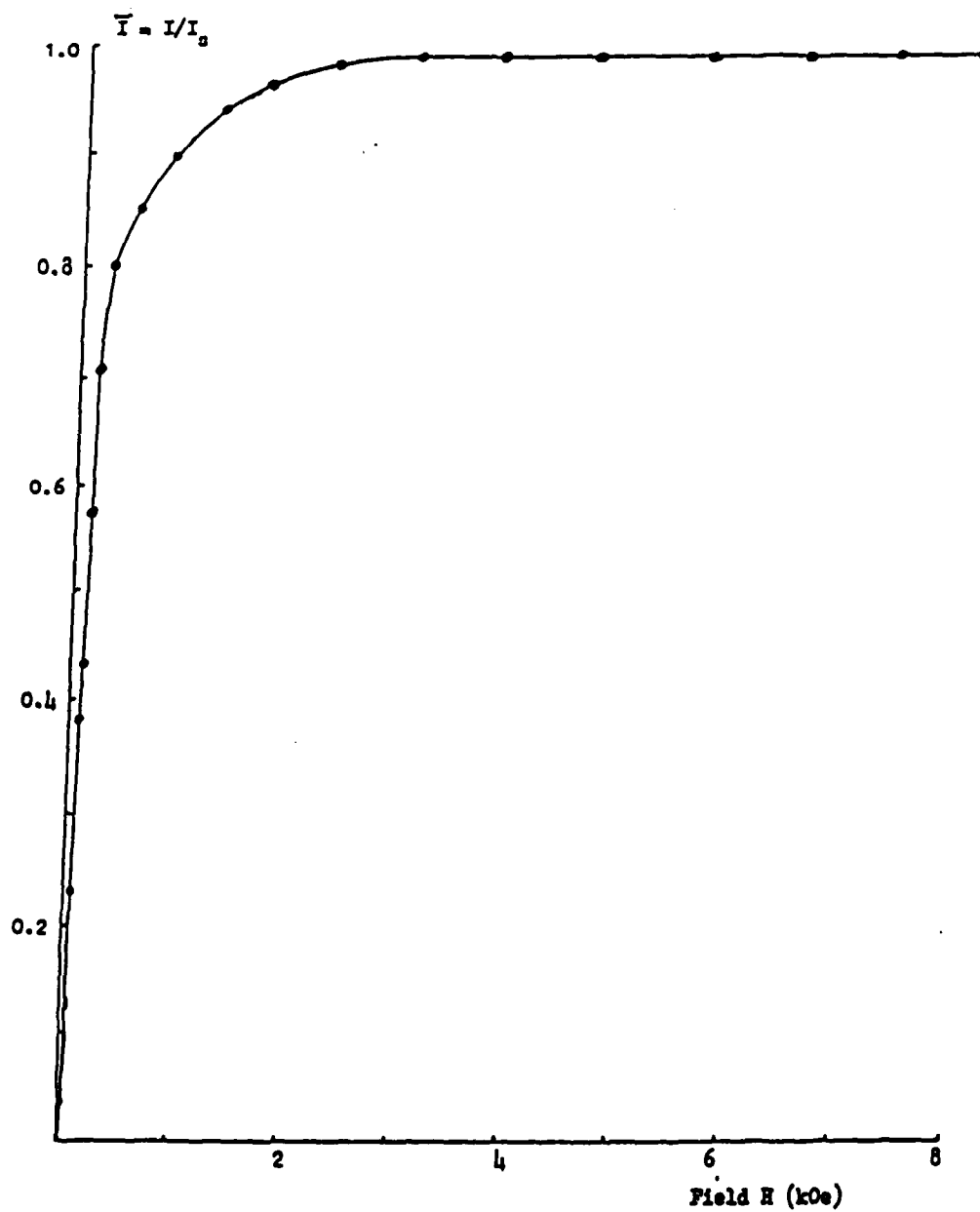


Figure 1 Room Temperature Magnetisation Curve of a 60 A  
Cobalt Ferrofluid

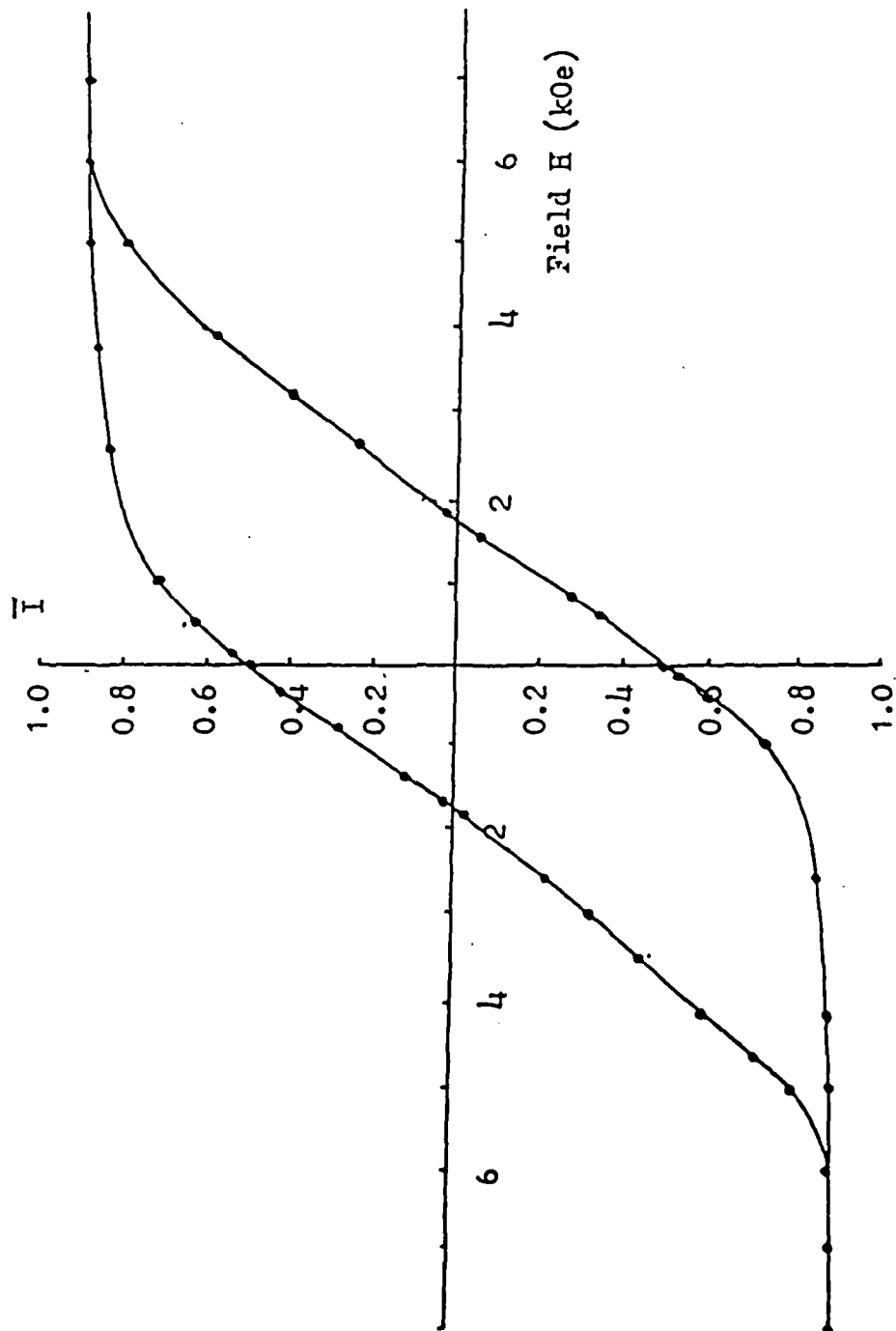


Figure 2 Low Temperature Magnetisation Curve of a 60 A Cobalt Ferrofluid

particles, however, with  $a \approx 25\text{\AA}$  can show superparamagnetic behaviour in both the liquid and solid states.

#### 2.1(b) The Magnetisation Curve

Although ferrofluids are superparamagnetic and each particle can be considered equivalent to a giant paramagnetic molecule the simple classical Langevin treatment of paramagnetism requires modification when applied to magnetic fluids. The Langevin treatment takes no account of magnetostatic interactions which are important for those particles of large magnetic moment found in magnetic fluids. The effect of magnetostatic interactions is to change the structure of the magnetic fluid by forming particle aggregates which may be chains in a magnetic field or ring or necklace arrangements in zero field. Aggregation can be prevented if the magnetostatic energy is less than the thermal energy  $kT$ . For two identical particles of magnetic moment  $\mu$  the magnetostatic energy

$$U = -2\mu^2/r^3 \quad (3)$$

where  $r$  is the interparticle separation and  $\mu = I_B V$ .

$|U|$  is greatest when  $r = 2a$  whence the condition for non aggregation becomes

$$(I_B V)^2/4a^3 < kT \quad (4)$$

This gives a minimum size for the particle radius below which aggregation would not be expected at temperature  $T$ . In a real system, however, not all the particles would have the same size and some aggregation between the larger particles would be expected. The 'quality' of a magnetic fluid can be measured by the degree of aggregation and clearly would be improved if the particle sizes were made very small and uniform.

## 2.2 Optical Properties of Magnetic Fluids

Magnetic fluids show a magnetic birefringence, dichroism and Faraday rotation. These effects arise from the magnetic particles within the fluids and in order to interpret observations it is necessary to know the particle size distribution parameters as well as the mode of magnetisation.

The Faraday rotation and associated ellipticity of a polarised beam occur when the magnetic field is parallel to the direction of propagation of the light. Both effects are small and the Faraday rotation is less than a degree in a magnetic fluid,  $\bar{M}_B = 4\pi\bar{I}_B = 10^{-4}G$ , diluted 1 part in  $10^6$  by volume to give good optical transmission. In contrast to Faraday rotation the birefringence and dichroism of a magnetic fluid of the same concentration but with the magnetic field perpendicular to the direction of propagation of the light are easy to measure and are relatively large effects.

The origin of the strong birefringence and dichroism is still uncertain but is unlikely to be due to crystalline anisotropy since it occurs with  $Fe_3O_4$  particles which have a cubic structure. A more likely explanation is that the optical anisotropy arises from particle alignment in the magnetic field and the presence of a shape anisotropy. In the simplest case the magnetic moment of the particle would lie along the long axis of an ellipsoidal particle (the easy direction) and the particle would align with the magnetic moment coupled to the magnetic field. The magnetic moment would need to be blocked and the mode of magnetisation would be by Brownian particle rotation. As with magnetic measurements any interpretation of data must take into account the particle size distribution. The

birefringence  $\Delta n$ , induced by an applied magnetic field is then given by Hartmann et al (1984).

$$\Delta n = \frac{\epsilon}{2n_0} (g_{\perp} - g_{\parallel}) \int_0^{\infty} \xi(q) f(y) \left[ 1 - \frac{3}{p} L(p) \right] dy \quad (5)$$

where  $\epsilon$  is the packing fraction of particles,  $n_0$  the isotropic refractive index,  $(g_{\perp} - g_{\parallel})$  the difference in optical polarizabilities perpendicular and parallel to the field,  $p = \mu H / kT$  and  $L(p)$  the Langevin function.  $\mu$  is the magnetic moment of the particle and  $\xi(q)$  is a coupling function which depends on the ratio of the energy barrier  $KV$  to the thermal energy ( $q = KV/kT$ ). In the two limiting cases when  $q = 0$  and  $q = \infty$ ,  $\xi(q) = 0$  and 1 respectively.  $f(y)$  is the particle size distribution function which is considered to be lognormal.

The dichroism is given by

$$\Delta k = \frac{\epsilon}{2n_0} (h_{\perp} - h_{\parallel}) \int_0^{\infty} \xi(q) f(y) \left[ 1 - L(p) \right] dy \quad (6)$$

where  $(h_{\perp} - h_{\parallel})$  measures the imaginary part of the optical polarisabilities.

For low fields Davies and Llewellyn (1979) have shown that

$$\Delta n = \frac{2\pi}{n_0} \epsilon (g_{\perp} - g_{\parallel}) \frac{I_0^2 H^2 \pi^2 D^6 (\exp 18 \sigma^2)}{540 k^2 T^2} \quad (7)$$

where  $\sigma$  is the standard deviation of the particle size distribution function and  $D$  is the median particle diameter. Good agreement between theory and experiment is apparent.

An alternative method for analysing optical properties is to undertake measurements in a pulsed magnetic field. For this experiment the sample is placed between crossed polarisers and then subjected to a pulsed magnetic field. Light is transmitted during the pulse but the intensity then reduces after the pulse is removed with a time constant which measures the rate at which the particles relax through Brownian motion. This relaxation time depends on the carrier viscosity and the particle size. The pulsed birefringence measurements should be compared with those of Bogardus et al. (1978) who made magnetisation measurements under similar pulsed conditions. The two decay curves are shown in Figure 3. Clearly a significant difference in the measurements is the absence of the fast relaxation process in the optical measurements. Short relaxation times are associated with Néel relaxation in the smaller particles present. Since no fast component is observed in the pulsed birefringence measurements it is tempting to conclude that only those particles which align in the magnetic field and in which the magnetisation is locked to the easy direction, contribute to the optical anisotropy. This conclusion is consistent with the observation that no magnetic birefringence or dichroism is observed in a cobalt particle ferrofluid where the mean particle radius is less than 25 Å and the relaxation processes are dominated by Néel rotation. For such particles the field coupling constant as measured by  $KV/kT$  is small and minimal alignment of the easy axes is expected.

Wiener in 1912 presented a simple theory which attributed the birefringence to shape anisotropy. This theory was later reviewed by Bragg and Pippard (1953) and modified by Llewellyn (1983) to include the effects of dichroism by including both real and

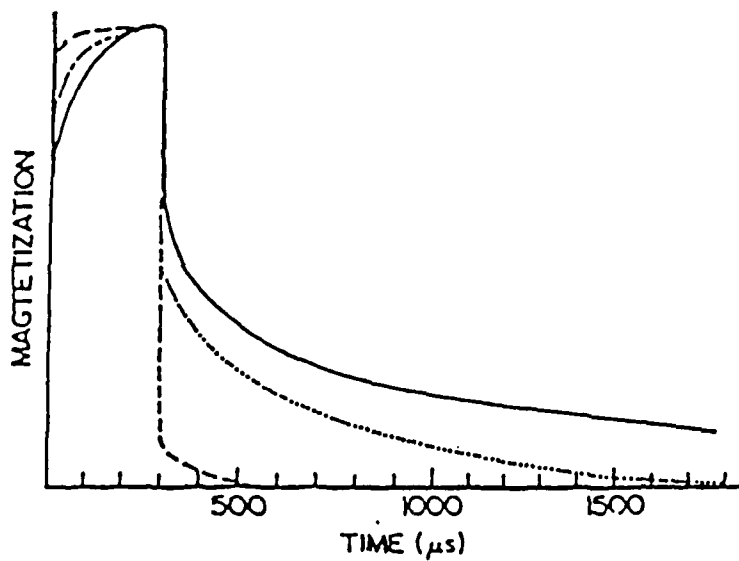


Figure 3 (i) Decay of magnetization with time

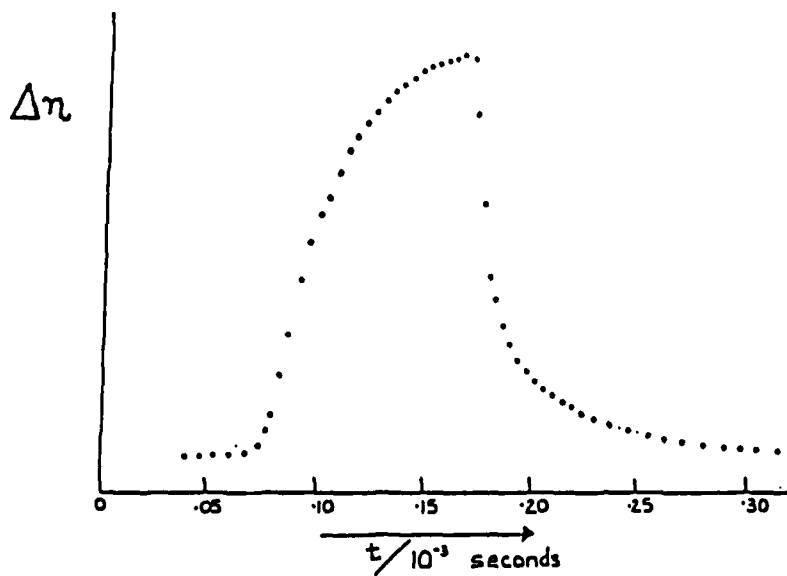


Figure 3 (ii) Decay of birefringence with time

imaginary parts of the refractive index in the analysis. It is thus possible to predict the variation of the birefringence and dichroism with wavelength for a specific particle elongation and concentration provided the refractive indices and absorption coefficients of both particles and carrier are known. Figure 4 shows the measured wavelength dependence of the birefringence and dichroism for a magnetic fluid containing cobalt particles in toluene. The birefringence  $\Delta n$  shows a change from negative to positive sign at a wavelength of 3700 Å. Such a change is predicted by theory and is related to particle shape. The theoretical and experimental curves can be matched by adjusting the particle concentration and elongation parameters. Good agreement is obtained if the particles are assumed to have an axial ratio 1.3:1 and  $\epsilon = 4 \times 10^{-6}$ . This shape anisotropy is rather larger than the predictions made from magnetic measurements and the concentration predicted is surprisingly small. Although the form of the wavelength dependence of the predicted birefringence and dichroism curves is encouraging the estimated values for the particle elongation and concentration require to be explained.

Because of particle interactions it is inevitable that some aggregates form in the magnetic fluid. These may be in the form of dimers or trimers and arise because there are always large particles present in a particle size distribution. These exist in the stock material before dilution and will continue to exist after dilution because of the strong magnetostatic interactions. These elongated clusters could well be responsible for the observed magnetic birefringence. This explanation would also account for the absence of a magnetic birefringence and dichroism in magnetic fluids containing very small 25 Å radius cobalt particles. Magnetostatic

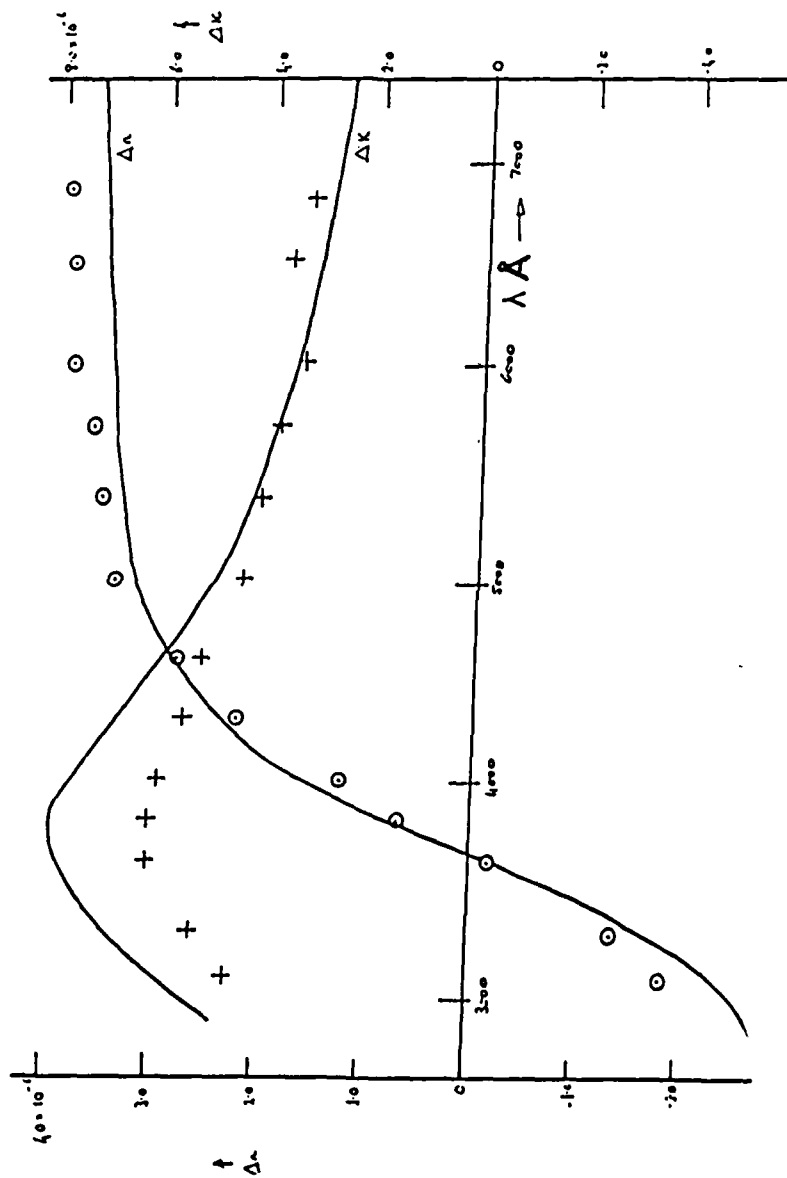


Figure 4 Wavelength Dependence of Optical Dichroism and Birefringence

interactions in this case are small and cluster formation is, therefore, unlikely. An alternative explanation is that the birefringence arises from isolated and unrepresentative elongated particles. The concentration of these would only need to be small ( $\epsilon = 4 \times 10^{-6}$ ) to give the required birefringence.

The birefringence in magnetic fluids has been studied recently using Monte-Carlo calculations (Chantrell et al 1984). This analysis shows that magnetostatic interactions between particles coupled to the field direction would lead to metastable aggregates and a consequent optical anisotropy. The magnitude of the effect is, however, uncertain.

There is currently no interpretation of the optical measurements which is unambiguous. More measurements are required on particle systems containing elongated particles and the effect of clusters has to be carefully evaluated. Unfortunately, it is difficult to produce magnetic fluids containing elongated particles in the size range 50 to 100 Å. Further studies are, however, continuing.

The optical and microwave properties of composites which have a ferrofluid base will inevitably contain a contribution from the ferrofluid itself. The optical contribution has already been discussed. The microwave properties have been studied recently by Birch et al (1985) who have observed measurable effects (dichroism, birefringence, and Faraday rotation) in the near millimetre range. These effects, however, are much smaller than those observed and measured in composites where the particle structures induced by the applied magnetic field dominate over the smaller contributions from the carrier fluid. The remainder of this Report will be concerned,

therefore, with the study of composites prepared and measured as part of a specific programme of research which is directed towards the production of materials that might find application in microwave devices in the near millimetre wavelength range.

### 3 MAGNETIC PROPERTIES OF FERROFLUID COMPOSITES

#### 3.1 Composites containing polystyrene spheres

Skjeltorp [1] has shown that in a magnetic field spherical polystyrene particles dispersed in a ferrofluid acquire a strong induced magnetic moment  $\underline{\mu}$  which can be written for small fields in terms of the effective magnetic fluid susceptibility  $\bar{\chi}_{eff}$ . Hence

$$\underline{\mu} = -\bar{\chi}_{eff}V\underline{H} \quad (8)$$

where  $V$  is the particle volume and  $H$  the applied field. In determining  $\bar{\chi}_{eff}$  demagnetising factors  $N_s$  and  $N_p$  arising from sample and particle shapes must be included. Thus

$$\bar{\chi}_{eff} = \chi / (1 + (N_s - N_p)\bar{\chi}) \quad (9)$$

where  $\bar{\chi}$  is the carrier fluid susceptibility. For a sample in the form of a monolayer of polystyrene spheres in a thin film of ferrofluid and with  $H$  parallel to the plane of the film  $N_s = 0$ . Thus,

$$\bar{\chi}_{eff} = \bar{\chi} / (1 - N_p\bar{\chi}) \quad (10)$$

$N_p = 4\pi/3$  for spherical particles.

The particles interact through a strong diamagnetic interaction which for two spherical particles separated by a distance  $r$  is given by

$$E = \mu^2(1 - 3 \cos^2\theta)/r^3 \quad (11)$$

where  $\theta$  is the angle between the magnetic field and the line of centres of the two particles. For the case where  $H$  is parallel to the plane of the film the minimum interaction energy is

$$E = -2\mu^2/r^3 \quad (12)$$

Equation (11) indicates that the interaction between spheres may be either attractive or repulsive depending on  $\theta$ . Equation (12) gives the attractive case ( $\theta = 0$ ) where the spheres form into chains

whilst for the repulsive situation ( $\theta = \pi/2$ ) and

$$E = \mu^2/r^3 \quad (13)$$

In this situation the spheres form a hexagonal or triangular lattice which may be destroyed if the thermal energy is too large. The two situations identified by equations (12) and (13) for the case when the thermal energy is small are shown in Figures 5 and 6.

Skjeltorp (1983) has defined a controlling parameter for the stability of the triangular lattice as

$$\Gamma(\theta) = \mu^2/r^3kT \quad (14)$$

which simply compares the magnetic to thermal energies. For  $\Gamma(\theta=90^\circ) > \Gamma_C = 63$ , that is for large fields or large diameter spheres the triangular lattice should be stable. Similarly for  $\Gamma(\theta) < \Gamma_C$  a disordered structure, analagous to that arising in melting, is expected. The chain length when the field is applied parallel to the surface layer depends on thermal effects for a composite with specified  $\bar{\chi}_{eff}$ , and particle radius  $a$  and applied magnetic field  $H$ . This is an important factor in the consideration of composites for microwave device applications where the chain length would decide the magnitude of any field dependent absorptions. The use of Monte-Carlo calculations as described later in this Report and Davies et al (1985) are valuable, therefore, when used to predict the extent of chaining in composite structures.

### 3.2 Relaxation effects in composite structures

Relaxation effects in composite structures have not been studied in detail though thermal effects are clearly important. Thermal effects are responsible for dispersing particles once the applied magnetic field has been removed.

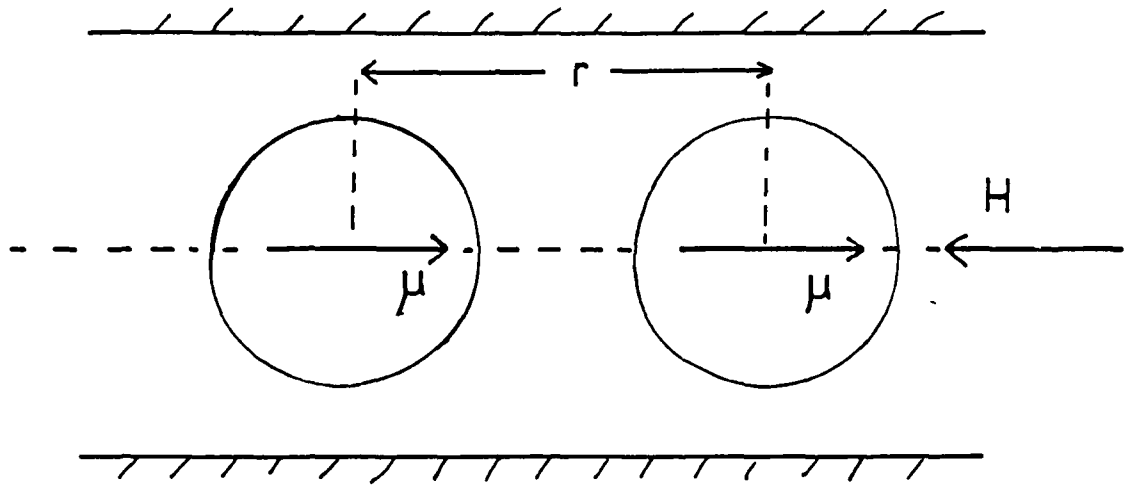


Figure 5 Interacting Polystyrene Spheres,  $H$  Parallel to Film

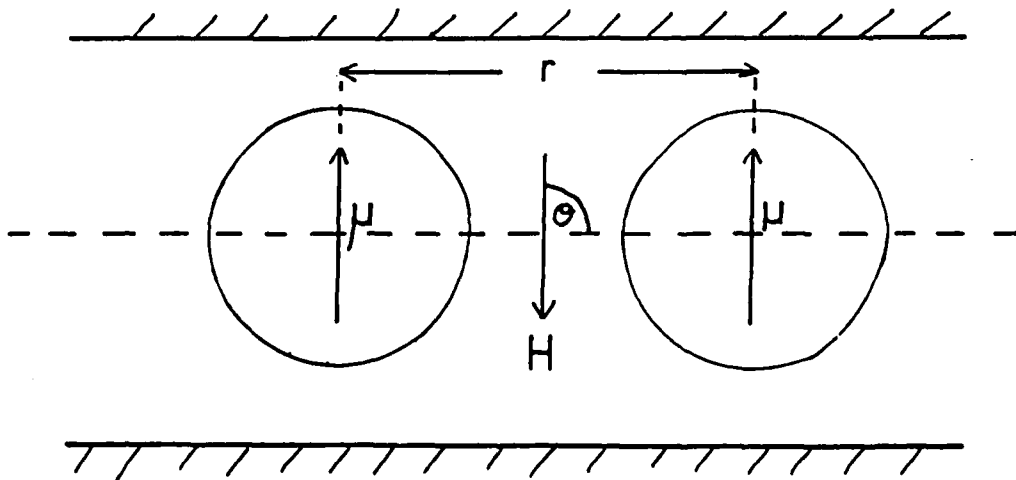


Figure 6 Interacting Polystyrene Spheres,  $H$  Perpendicular to Film

Using the Einstein relation

$$D = kT/6\pi\eta a \quad (15)$$

for the diffusion coefficient an estimate of the distance moved,  $x$ , as part of a random walk process can be calculated from

$$x \approx \sqrt{Dt} \quad (16)$$

giving

$$x \approx \sqrt{\frac{kT}{6\pi\eta a}} \cdot t \quad (17)$$

implying that a particle of diameter  $10^{-3}$ cm would travel  $10^{-5}$ cm in 1 sec, that is 0.01 of a particle diameter. Diffusional mixing is therefore very small and other processes would seem to be responsible for the changes in composite structure which are observed immediately the applied field is removed. These relaxation processes are discussed in more detail together with experimental observations in Section 5.1.(c).

#### 4 EXPERIMENTAL PROCEDURE

##### 4.1 Preparation of the composite carrier ferrofluids containing magnetite particles

The method used for producing surfactant coated magnetite was based on that given by Shimoizaka et al (1980). Sodium oleate coated particles of magnetite ( $\text{Fe}_3\text{O}_4$ ), approximately 100 Å in diameter were prepared in the following way. The reaction mechanism is shown in Figure 7.

A mixture of 130 g of ferric chloride and 77 g of ferrous sulphate (molar ratio 2:1) was dissolved in distilled water. The resulting solution was highly acidic (pH 2) and approximately 400 ml of 10 M sodium hydroxide solution was added until the pH had risen to a value of about 11. The solution was stirred for an hour at room temperature to form the  $\text{Fe}_3\text{O}_4$  precipitate. An excess amount (21 ml) of oleic acid ( $\text{CH}_3(\text{CH}_2)_7 \text{C}-\text{C}(\text{CH}_2)_7 \text{C} \begin{smallmatrix} \text{O} \\ \parallel \\ \text{OH} \end{smallmatrix}$ ) was added to the mixture. In these alkaline conditions the acid dissociates due to the presence of sodium ions, and thus the oleate ion is free in solution. The oleate ions were chemisorbed onto  $\text{Fe}^{2+}$  ions at the surface of the magnetite particles and since an excess was present complete coating was ensured. Physisorption between sodium oleate molecules also occurs and forms a partial second layer over the magnetite (Figure 8).

Nitric acid was added until the pH was approximately 4.5 and the mixture was heated to  $100^\circ\text{C}$ . This coagulated the magnetite by converting the oleate ion in the second layer to hydrophobic free acid molecules. The coagulate was repeatedly washed in acetone and distilled water to produce magnetite coated with a monolayer of oleate. The magnetite was then dried under vacuum and dispersed in an appropriate carrier liquid.

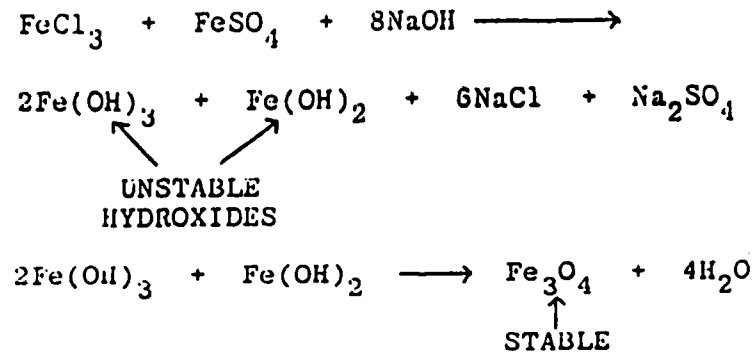


Figure 7 Reaction Mechanism for Producing Magnetite Particles

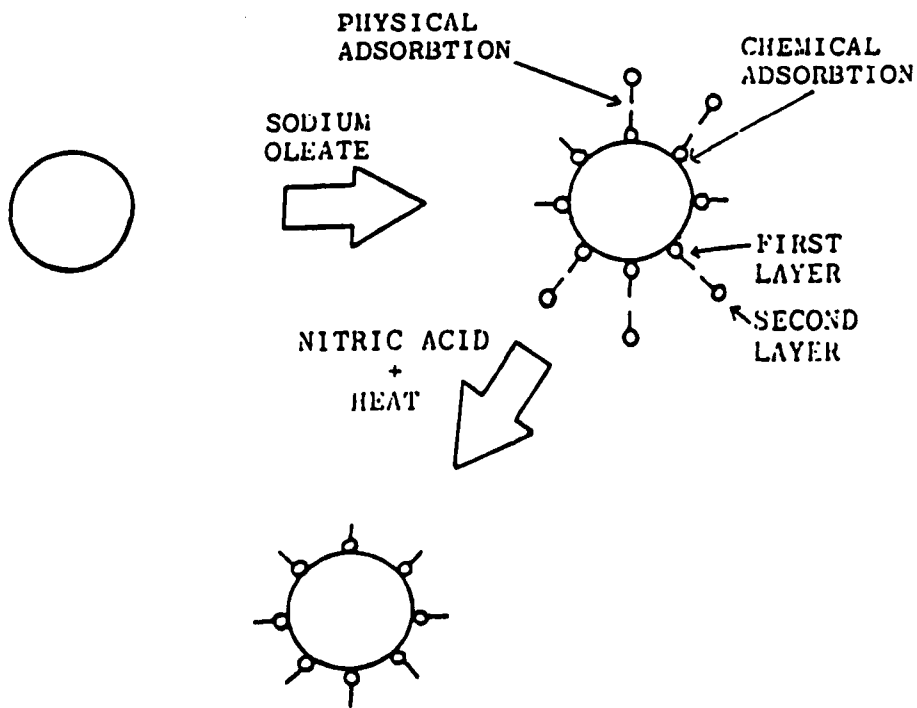


Figure 8 Surfactant Coating of Magnetite Particles

Two liquids have been used as carriers, isopar M and decalin. To disperse the magnetite powder 5 ml of the required carrier liquid was placed in a small beaker. The carrier was gently heated and about 0.25 g of the oleic coated magnetite was added and continually stirred to disperse the powder. By altering the amount of magnetite added to the carrier the saturation magnetisation,  $I_s$ , of the resulting fluid was varied.

To ensure that the fluids did not contain large agglomerates which would lead to colloidal instability they were finally centrifuged at 3500 rpm for 30 minutes. The top 75% of the resulting colloid was then decanted off and the residue discarded.

#### 4.2 Preparation of Ferrofluid Composites

##### 4.2 (a) Preparation of samples containing polystyrene spheres for optical studies

The composite colloid samples were made using the method given by Skjeltorp (1983). A typical sample containing 1  $\mu\text{m}$  diameter polystyrene spheres dispersed in an Isopar M based magnetic fluid (prepared as described in Section 4.1) was made as follows. A few drops of an aqueous suspension of polystyrene spheres were placed on a clean, dust-free microscope slide and the water allowed to evaporate. One drop of ferrofluid was then pipetted onto the slide and a glass cover slip placed on top. The cover slip was pressed down to displace any excess ferrofluid and to form a monolayer of spheres. It was also necessary to move the cover slip in a circular motion to dislodge any spheres that might have become attached to the microscope slide. The sample was then sealed using an epoxy resin to prevent the carrier liquid evaporating (Figure 9). By varying the amount of the aqueous suspension of polystyrene spheres placed on

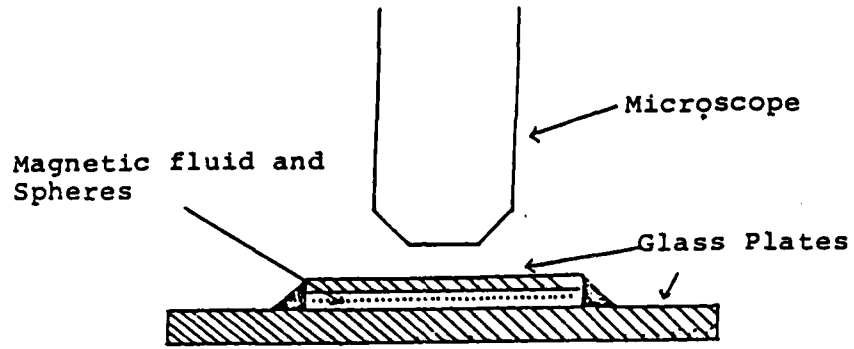


Figure 9 Composite Colloid Sample

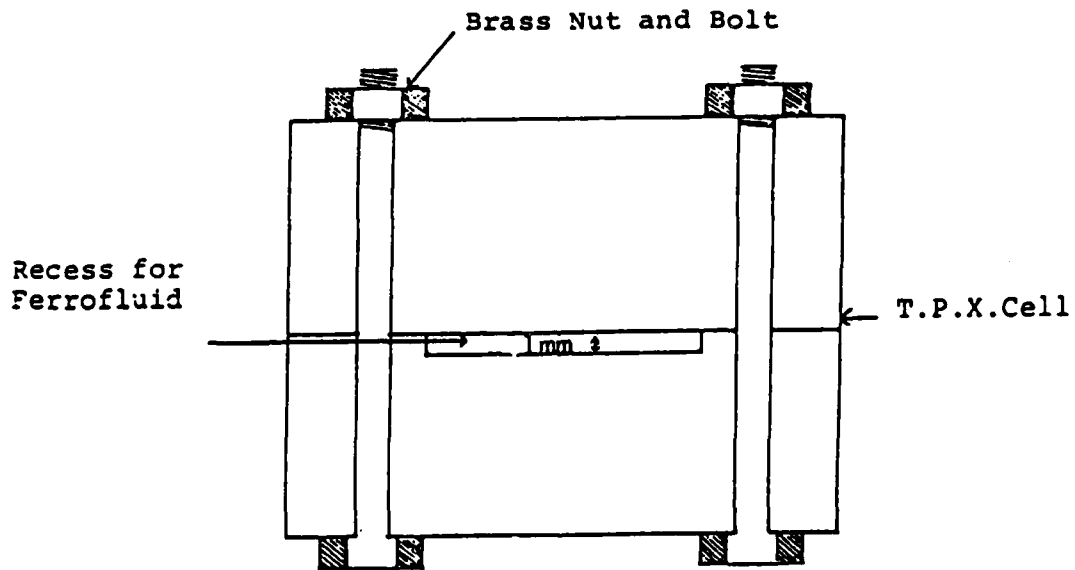


Figure 10 Cell for Microwave Measurements

the microscope slide samples of different concentrations could be produced.

#### 4.2 (b) Preparation of samples containing non-magnetic metallic particles for optical studies

The method of preparing composites containing metallic particles was very similar to that described in the previous Section 4.2 (a). However, the metallic particles were not in aqueous suspension but in the form of a dry powder. They were, therefore, dusted onto the glass microscope slide through a fine gauze. Ferrofluid was then pipetted onto the slide and a cover slip placed on top and the sample sealed.

The methods by which particle concentrations were measured are discussed later in Section 4.2 (c).

The samples were examined with a Swift MP120 polarizing microscope with camera tube attachment (Figure 9). External fields of up to 100 Oersteds could be applied to the samples using either a Helmholtz pair of coils or permanent magnets.

#### 4.2 (c) Preparation of samples for microwave measurements

Two types of microwave samples were produced, one for use with the single wavelength microwave 3mm source and the other for use in the broad band Fourier Transform Spectrometer (Sections 4.3 (a) and 4.3 (b) respectively). All the samples contained metallic particles. No significant microwave effects were noticed from a composite containing polystyrene particles.

Glass was not used in the construction of the sample cell for single frequency measurements since it is highly absorbing at wavelengths in the millimetre range. A good material to use is TFX (Chantry et al (1969)) which readily transmits in the wavelength

range above  $\lambda = 200 \mu\text{m}$ . Such a cell with a path length of 1 mm is shown in Figure 10.

Many samples were studied using different concentrations of non-magnetic metallic particles in a 375 Gauss Isopar M based ferrofluid. The particle concentration  $c$  of a sample was calculated as the total volume of the particles per ml of ferrofluid. To prepare a sample the particles were first weighed and then added to a known volume of ferrofluid. The two components of the system were mixed thoroughly and then syringed into the TPX cell. Extreme care was taken to ensure that no air bubbles were present in the cell before sealing the cell with a plug. The sample was then placed in the microwave system (Section 4.3(a)) for further investigation.

Although Isopar M absorbs 3 mm radiation the power output of the microwave source was such that no problems occurred in using a cell with a relatively long path length of 1 mm.

#### 4.2 (d) Preparation of microwave samples using z-cut crystalline quartz plates

Unlike the single wavelength 3 mm source, the mercury lamp used as the broad band source for Fourier Transform Spectroscopy has a much lower output in the millimetre and submillimetre region. This meant that the samples used in this section of the work had fundamental differences from those described in 4.2 (c) above. First the carrier liquid had to be changed to decalin which is a liquid with a low absorption in the near millimetre wavelength range. Second the path length of the sample had to be reduced. In fact, for this section of the work it was found that monolayers of the non-magnetic metallic particles in a thin film of the decalin based  $\text{Fe}_3\text{O}_4$  ferrofluid were ideal. These samples were made using precisely the same technique as that described in Section 4.2 (b). However, as

noted in Section 4.2 (c), glass plates absorb heavily in the millimetre wavelength region and so Z-cut crystalline quartz plates were used in place of the glass slides. Since the samples were true monolayers their concentrations were measured in terms of the number of particles per square centimetre. These concentrations were measured using optical microscopy techniques.

#### 4.3 Microwave Experiments

##### 4.3 (a) Single Wavelength ( $\lambda = 3$ mm) Experiments

The 3 mm wavelength apparatus used is shown in Figure 11. The source used was an Impatt diode, its name derived from the initial letters of Impatt Avalanche Transit Time. The Impatt diode is a specially doped p-n junction diode which is biased in the reverse direction so that a very high electric field intensity exists across a narrow region at the junction. Avalanche breakdown occurs in this narrow region and causes oscillation in the microwave range of frequencies. The polarized radiation from the source is polarised. A TPX lens focussed radiation from the source on to the sample which was in the form of a monolayer film with the plane of the film horizontal. Two sets of Helmholtz coils produced fields at right angles to one another in the horizontal plane and thus enabled the particle chains to be aligned either parallel or perpendicular to the plane of polarization of the source. The radiation passed through the sample and was turned through  $90^\circ$  using a front aluminised mirror. This was done purely for experimental convenience since the beam was then parallel to the laboratory bench. A second TPX lens focussed the beam on to the Golay pneumatic cell, the principal of operation of which is described in detail by Golay (1947, 1949).

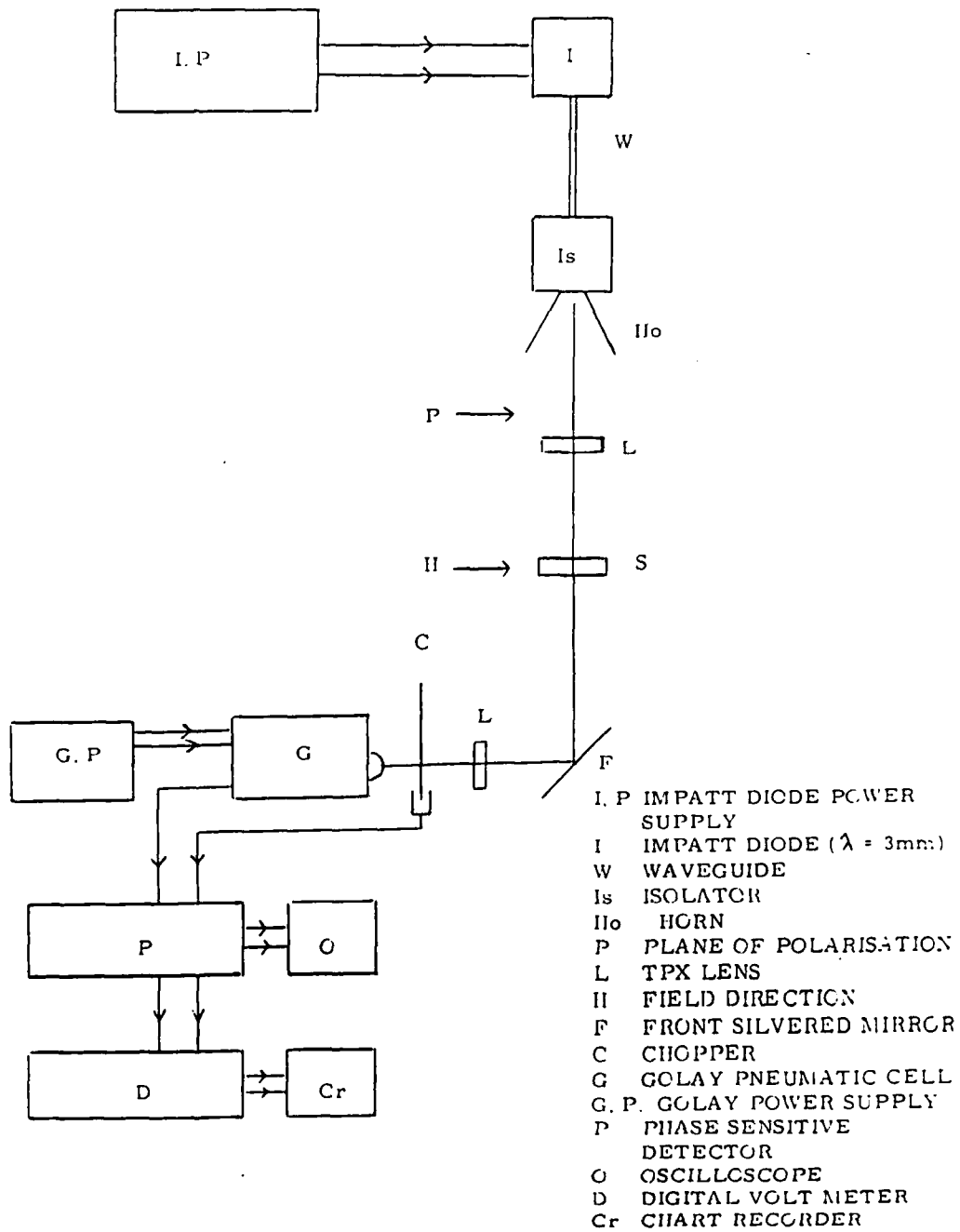


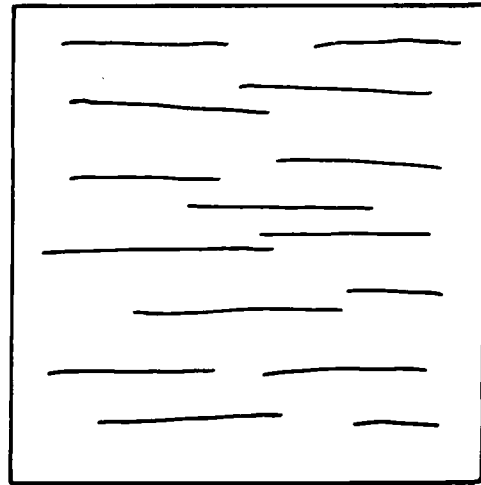
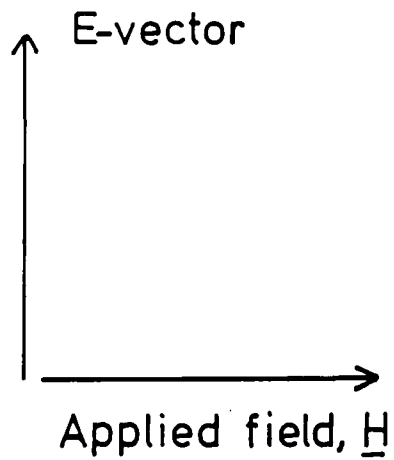
Figure 11 3 mm Wavelength Microwave Apparatus

The light beam was modulated using a chopper at 13 Hz and the output signal from the Golay cell was passed to a lock-in amplifier. The resulting dc signal was directly proportional to the intensity of the radiation falling on the detector.

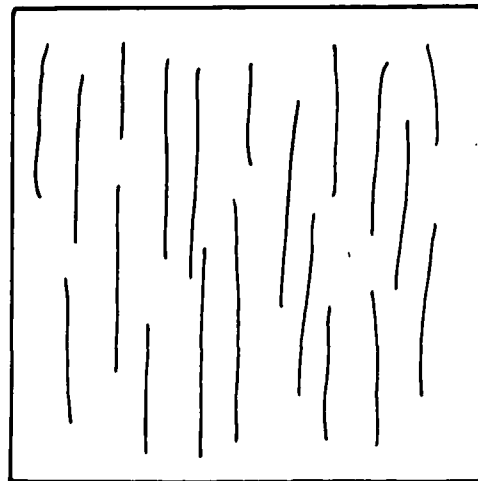
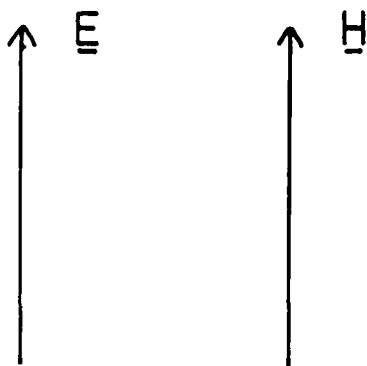
It is important in this experiment to ensure that the initial state, that is the form of the composite before the application of a magnetic field, was reproducible. Because relaxation effects have a time constant of many minutes an initial state corresponding to a random array of particles was unrealistic and could not be readily achieved once a magnetic field has been applied. To overcome this problem a saturating field of 70 Oe was applied to the sample perpendicular to the plane of polarisation of the incident beam. This aligned the particle chains in the composite and the transmitted intensity  $I_0$  at this stage was measured Figure 12. The magnetic field was removed and then applied parallel to the plane of polarisation of the microwave source and the transmitted intensity  $I$  measured as a function of the applied field. The transmission  $T$  of the sample, defined as  $T = I/I_0$ , was plotted as a function of the field,  $H$ . The smallest value of transmission measured in the field was defined as  $T_f = (I/I_0)_{\text{final}}$ . This would be the value corresponding to the situation when all the chains were aligned in the field direction. With this procedure the initial state is always recoverable and comparisons with other samples can readily be made. It must be noted, however, that the absorptions recorded in this experiment are greater than would be expected from an unpolarised source.

Experiments are also being undertaken to measure quantitatively the magnetic dichroism and birefringence at microwave

composites containing  
chained particles



initial measurement  
of  $I_0$



subsequent measurement  
of  $I$

Figure 12 Different Field Orientations for the Measurement  
of  $I_0$  and  $I$

wavelengths. The experimental set-up as shown in Figure 13 contains two additional polarizers. The first, which is needed to measure the dichroism polarised the beam at 45° degrees to the applied field. This produced two equal components of radiation  $I_V$  and  $I_H$  at 90° to each other. The large field induced dichroism is then given by the expression

$$\Delta A = \log_{10} (I_H/I_V) \quad (18)$$

where  $I_H$  is the transmitted intensity of the radiation polarized in the field direction and  $I_V$  the transmitted intensity perpendicular to the field direction. A second polarizer measured the change in polarisation of each component and from this the magnetic birefringence present in the sample could be determined.

An initial study of the relaxation of these systems on the removal of a magnetic field (Section 3.2) was also undertaken using the same experimental arrangement described in 4.3 (a). A sample whose transmission had previously been measured was left in a saturating field of about 300 Oe parallel to the plane of polarization of the incident radiation. The relaxation of the particle chains after the field was removed was then studied by measuring the change in the intensity of the transmitted radiation,  $I$  as a function of time. The results are presented in Section 5.

#### 4.3 (b) Fourier Transform Spectroscopy (FTS)

Preliminary measurements have been made on monolayer ferrofluid composites (Section 4.2 (d)) using FTS. Since the Fourier Transform Spectrometer records simultaneously all the elements of the spectrum (the multiplex advantage) it enables the field induced absorption to be studied as a function of wavelength.

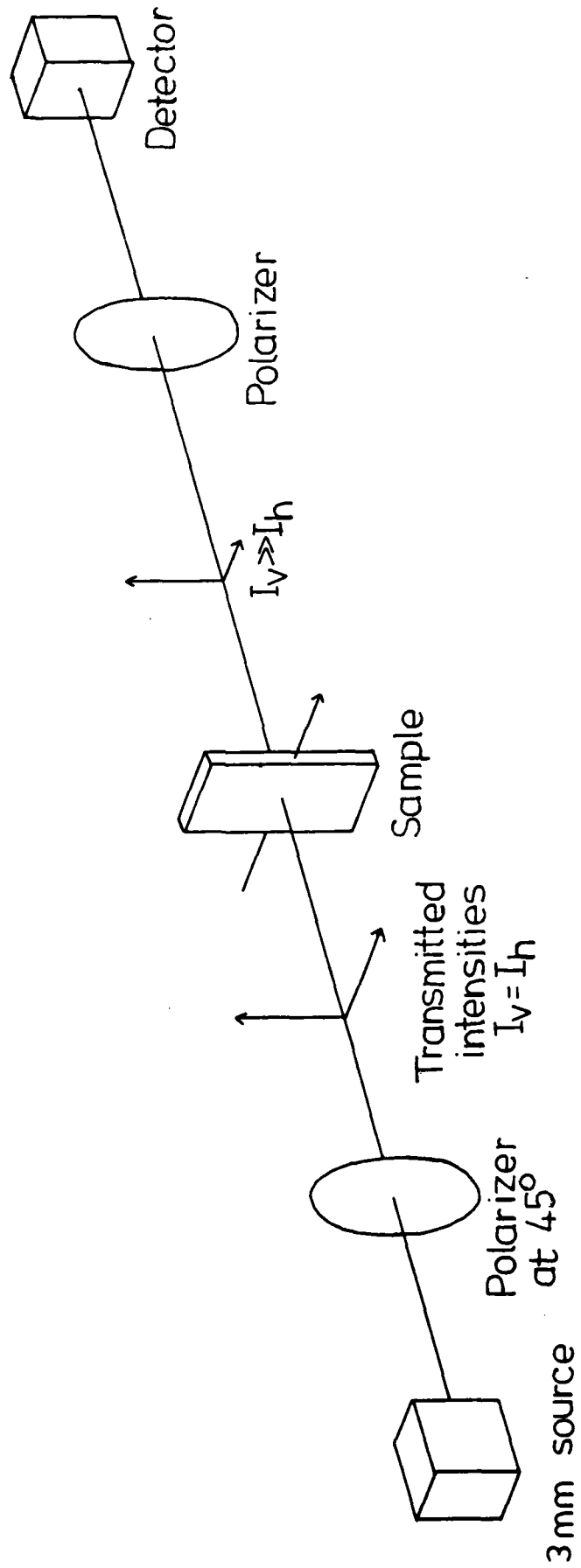
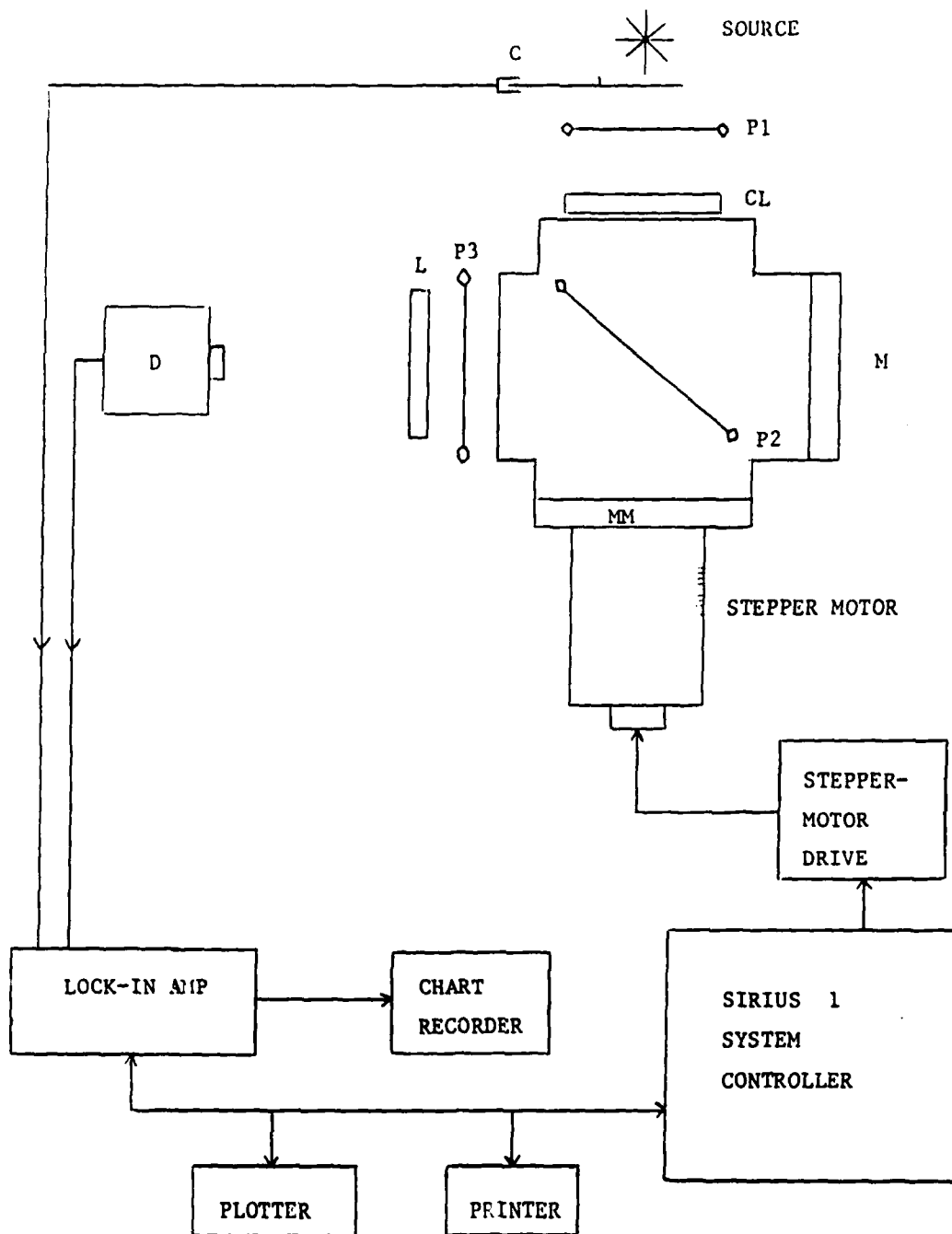


Figure 13 Apparatus for Measuring Dichroism and Birefringence at Millimetre Wavelengths

The Fourier Transform Spectrometer used to study monolayers of composite colloids is shown in Figure 14. It is clearly desirable to choose a spectroscopic system giving an optimum transfer of energy from the source to the detector. Such a system uses a two-beam Michelson interferometer which has the highest throughput of any spectroscopic system.

Radiation from the water cooled mercury lamp source was passed into the interferometer via a polarizer P1. The resulting plane polarized radiation was then split into two components using the beam splitter, P2. One beam was reflected back to P2 by a stationary mirror M, the other by the movable mirror MM. At P2 the beams recombined with their respective planes of polarization at  $90^\circ$  to each other. In order for these to interfere their planes of polarization were made parallel by polarizer P3. The two beams were then focussed on the sample S using a TPX lens L before entering the detector R which was a helium cooled Rollin detector (Rollin (1961), Kinch and Rollin (1963)) rather than the Golay pneumatic cell used in Section 4.3 (a). This was due to the lower output of the mercury lamp compared with that of the Impatt diode and the fact that the Rollin detector was more sensitive to millimetre and submillimetre radiation than the Golay cell. The output was linked to a phase sensitive detector (PSD) and the radiation was modulated using a chopper which provided the reference for the PSD. The whole spectrometer was interfaced (Jefferies et al (1984)) to a Sirius microcomputer which collected all data. An interferogram with amplitude modulation is shown in Figure 15.

A typical measurement on a monolayer sample was made as follows. A sample of the form of a monolayer was placed in the



C - CHOPPER  
 P1, P2, P3 - POLARIZERS  
 CL - COLLIMATING LENS  
 M - FIXED MIRROR  
 MM - MOVEABLE MIRROR  
 L - FOCUSSING LENS  
 D - DETECTOR

Figure 14 The Fourier Transform Spectrometer

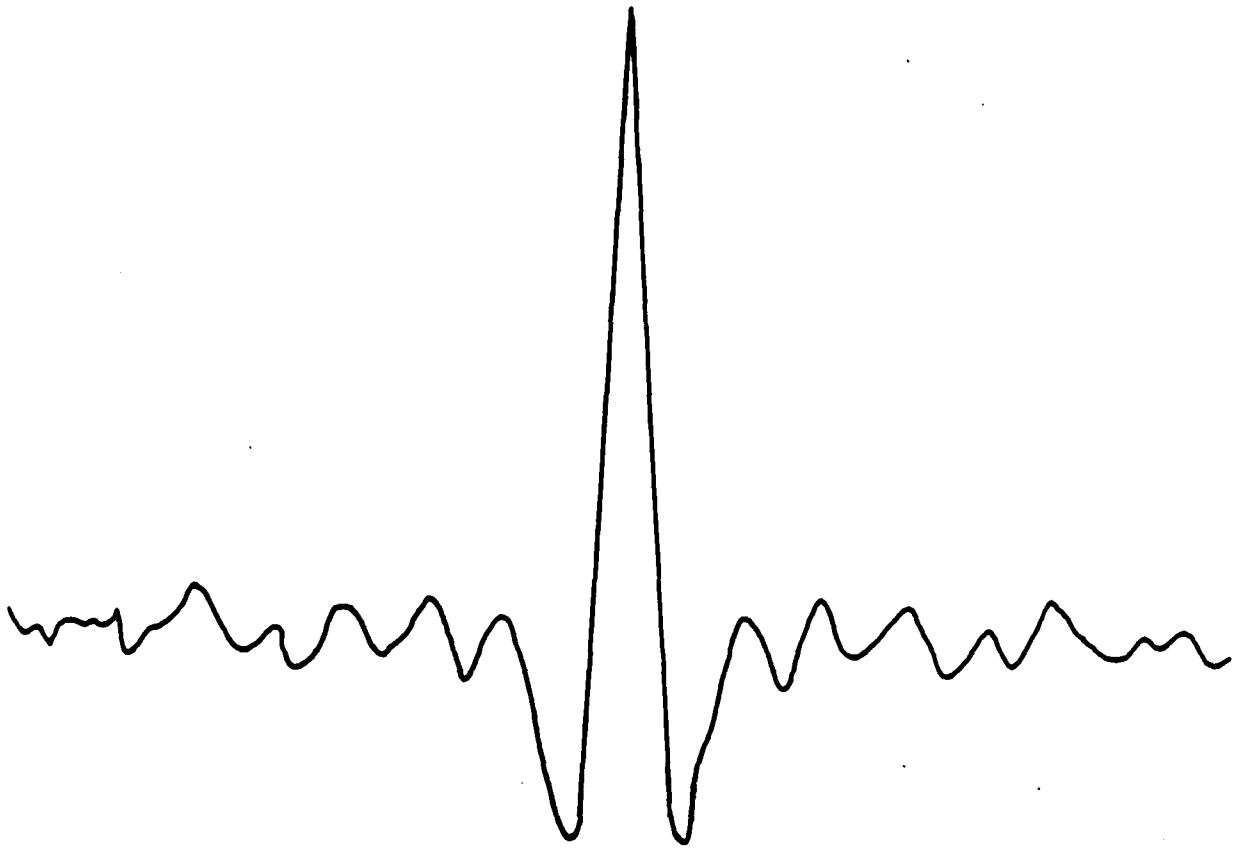


Figure 15      An Amplitude Modulated Interferogram

interferometer as shown in Figure 14 and a scan made with a small magnetic field, approximately 50 Oe, applied in a direction perpendicular to the plane of polarization of the incident radiation. This was taken as the reference scan, analogous to  $I_0$  in Section 4.3 (a). A second field of about the same size was then applied parallel to the plane of polarization of the incident radiation to align the particle chains in the sample in the same direction. This produced a reduction in transmitted intensity and a scan was made with the field in this orientation. The resulting two interferograms were transformed by the computer into reference and sample spectra respectively and the ratio of the two spectra gave a plot of the transmission versus wavelength. Thus if no absorption was present the two spectra would be identical and the transmission unity at all values of wavelength. Any reduction in the transmission was the result of absorption by the ferrofluid composite. The results from a preliminary study are shown in Section 5.

#### 4.4 Monte-Carlo Simulations

The basis of the Monte-Carlo model as applied to magnetic fluids is described in detail by Chantrell et al (1980), Menear (1984) and Menear et al (1984). For a colloidal system in which Van der Waals forces are small the energy of a particle is given by Chantrell et al (1980) as

$$E_i = E_m + E_r + E_H \quad (19)$$

$E_m$  is the magnetostatic energy,  $E_r$  the energy due to repulsive forces arising from a surfactant coating and  $E_H$  the magnetic dipole energy of a magnetic particle in an applied magnetic field  $H$ . In the case of composites containing  $1\mu\text{m}$  diameter polystyrene spheres dispersed

in a ferrofluid, magnetostatic interactions are dominant. Thus equation 19 reduces to

$$E_i = E_m + E_H \quad (20)$$

since  $E_r$  is negligible compared with  $E_m$  and  $E_H$ .  $E_H$  is given by

$$E_H = -\mu H \cos \theta_1 \quad (21)$$

where the particle magnetic moment  $\mu$  is given by equation (8) and  $\theta_1$  is the angle between the magnetic moment of the particle and the direction of the applied field. Since the induced magnetic moment  $\mu$  of a polystyrene sphere is diamagnetic the moment is anti-parallel to  $H$  and  $\cos \theta_1 = -1$ .  $\mu$  has a value which depends on the applied field and the magnetization curve of the carrier fluid and is a constant if the magnetic field applied is sufficient to saturate the ferrofluid. Below saturation  $\mu$  is field dependent. The Monte-Carlo configurations in this section assume the field applied is fixed and large enough to saturate the carrier ferrofluid.

In the model used the initial random configuration of  $N$  polystyrene spheres ( $d = 1\mu\text{m}$ ) was confined to a square cell of side  $50\mu\text{m}$ . Each particle was subjected to a random displacement which was restricted to less than five particle diameters. The energy  $E_i$  of the particle was calculated in its new position and then compared with its original value. If the energy difference  $\Delta E_i \leq 0$  then the move was allowed. If  $\Delta E_i$  was positive a random number  $X$  was generated ( $0 \leq X \leq 1$ ) and compared with the value of  $\exp(-\Delta E_i/kT)$ . If the exponential was greater than  $X$  the move was allowed otherwise the move was prohibited and the particle returned to its original position. The energy of the system was computed after each move and when this reached an equilibrium value representing a final state the program was terminated. Periodic boundary conditions were used for

this analysis. The configurations generated by the above model are shown in Section 5.2 (a).

#### 4.4 (a) The Spatial Distribution Function

Evaluation of the spatial distribution function of a given Monte-Carlo configuration enables the extent of particle chaining to be determined. The spatial distribution function  $g(r,\theta)$  was defined as the average number of particles per unit area at a distance  $r$  and angle  $\theta$  from the origin (the centre of the reference particle), normalised by dividing by the average particle density  $\rho_0$ . The functions  $g(r,\theta)$  (shown in Section 5.2 (b)) were especially useful in determining the extent of spatial anisotropy in the system.

## 5. RESULTS

### 5.1 Magnetically induced Microwave Absorption Effects

#### 5.1 (a) Single frequency source

The transmission,  $T = I/I_0$ , through a composite film containing micron-sized tin particles dispersed in an  $Fe_3O_4$  Isopar M ferrofluid ( $M_g = 375G$ ) is shown in Figure 16 for different magnetic fields applied parallel to the plane of the film. The experimental arrangement is described in Section 4.1. Six plots have been drawn on the same axes, showing the variation in the absorption characteristics with the concentration of tin particles. It is clear that as the concentration is increased from  $c = 0.034$  to  $c = 0.410$  the absorption progressively increases. It should also be noted that a relatively large absorption is observed in a very low field ( $\approx 50$  Oe). This is an important factor as regards the usefulness of the composites in microwave devices.

The final transmission is defined as  $T_f = (I/I_0)_{final}$  and it is the condition which gives maximum absorption; it occurs in fields,  $> 50$  Oe, as can be seen from Figure 16. This is the condition of saturation when all the particles are aligned in chains. The final transmission  $T_f$ , plotted against particle concentration on a logarithmic scale, decreases exponentially with the particle concentration  $c$ , as shown in Figure 17.

$$\text{Thus } I = I_0 \exp(-k(H)c) \quad (22)$$

for a cell of fixed path length of 1 mm. For the case of  $H > 50$  Oe  $k(H)$  reaches a limiting value and equation (22) can be simplified to

$$I = I_0 \exp(-kc) \quad (23)$$

where  $k$  is a field induced absorption coefficient corresponding to complete chain alignment and  $c$  is the dimensionless particle concentration (Section 1).

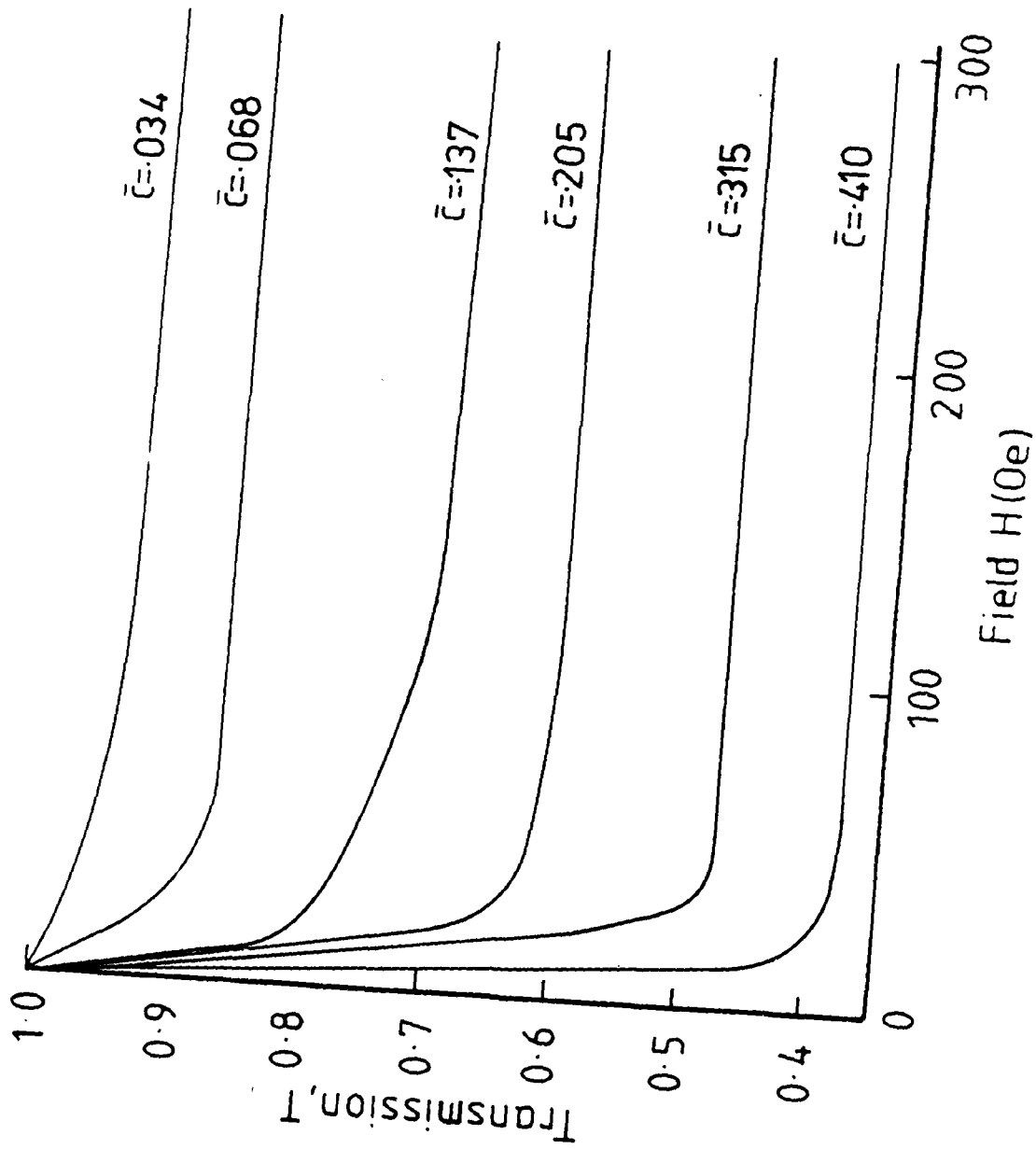


Figure 16 Plot of Transmission versus Field for Tin Particles

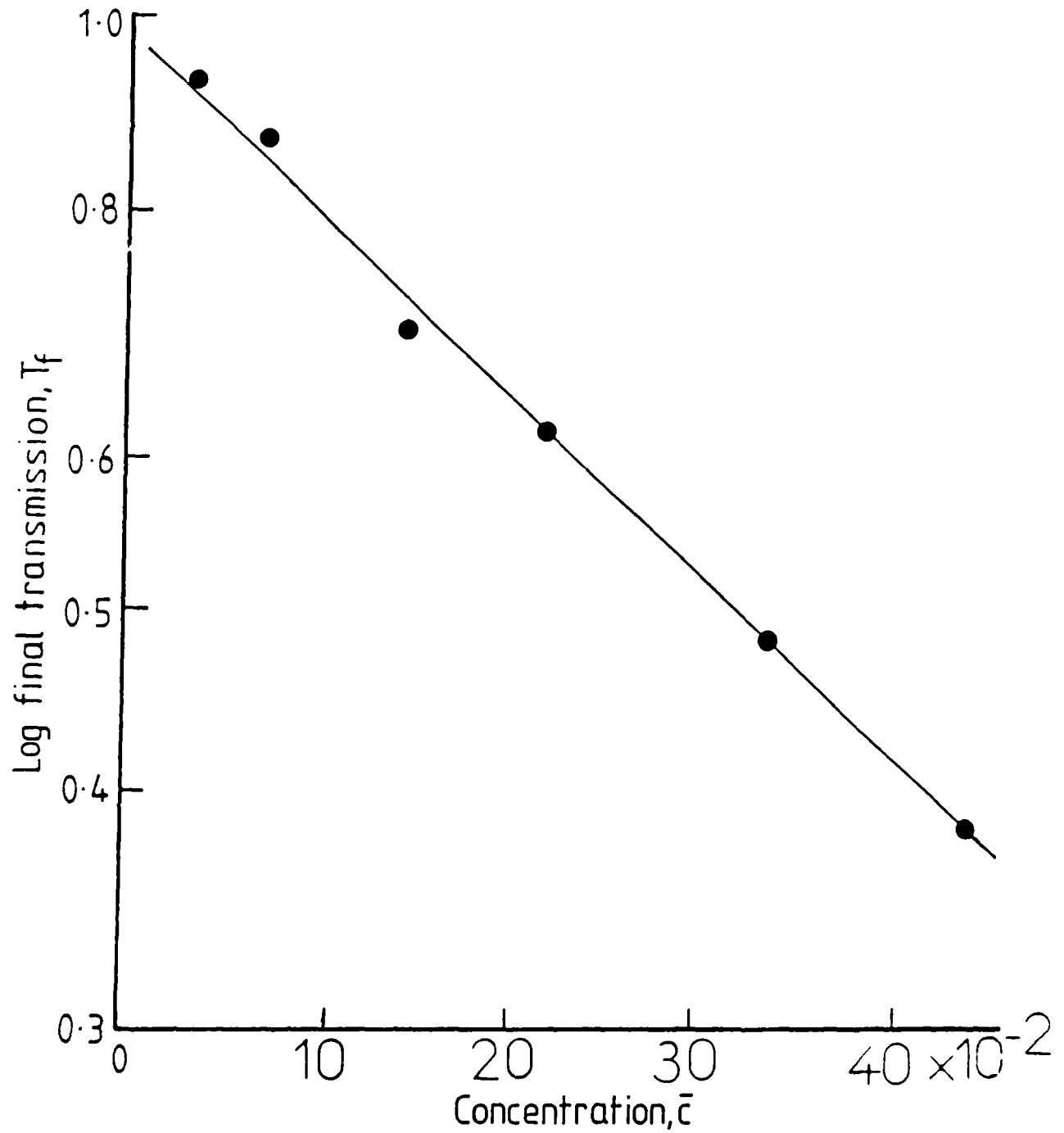


Figure 17 Plot of Final Transmission,  $T_f$  versus  
Concentration for Tin Particles

Composites containing conducting particles of other materials in the same 375G ferrofluid have also been prepared and examined. The final transmission/concentration characteristics, obtained by plotting  $\log_e T_f$  against  $\log_e c$  are shown in Figure 18 for silver, tin, carbon, copper and aluminium particles. As can be seen for these samples aluminium particles show the largest absorption whilst silver particles show the lowest.

Table 1 gives the values of  $k$  determined from Figure 3 and equation (23). It should be noted that high values of  $k$  are associated with composites giving a large absorption, that is they have a large absorption in fields greater than 50 Oe.

Table 1

MATERIAL		FIELD INDUCED
		ABSORPTION COEFF, $k$
Silver	(Ag)	0.38
Tin	(Sn)	2.37
Carbon	(C)	3.28
(graphite)		
Copper	(Cu)	4.92
Aluminium	(Al)	6.11

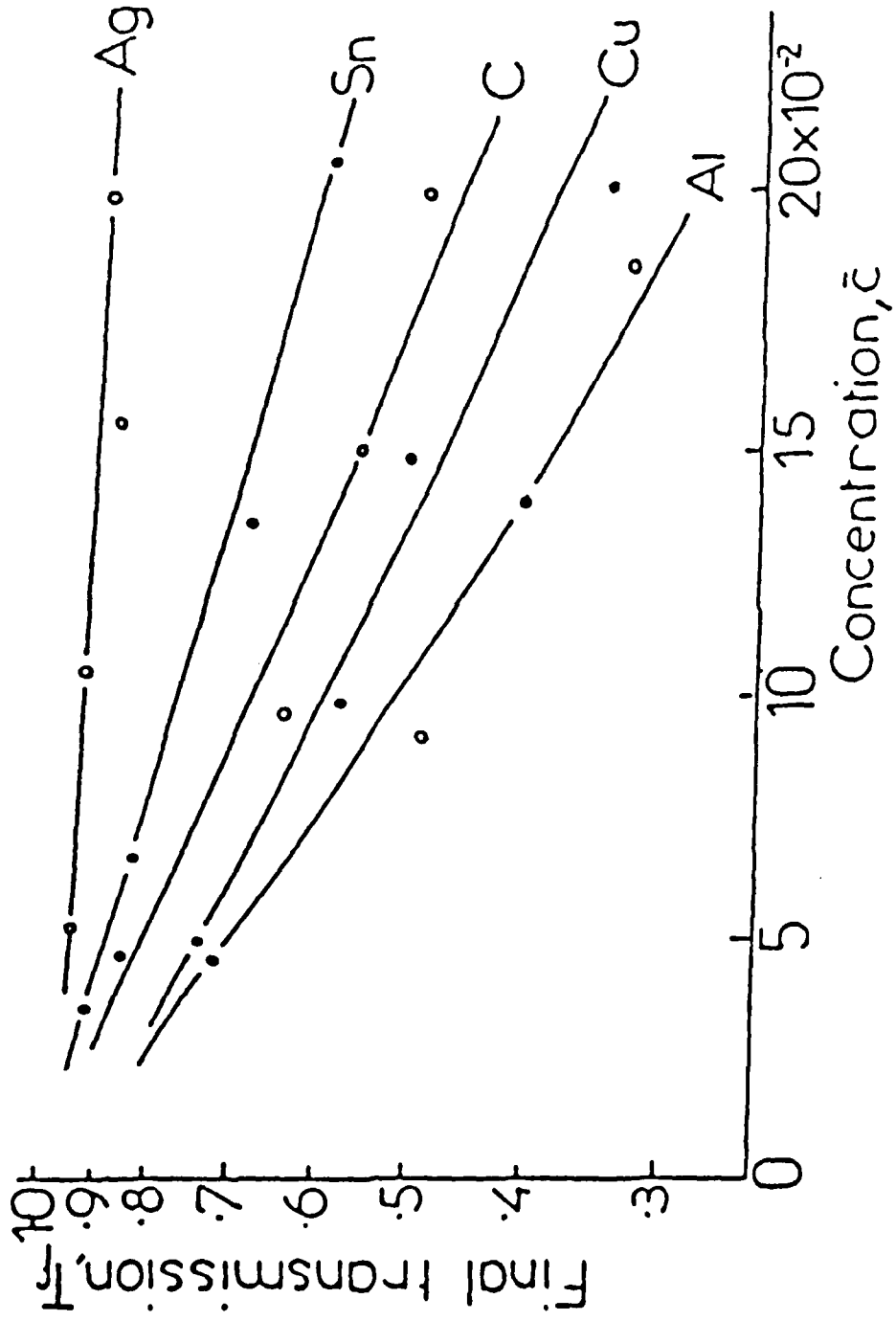


Figure 18  $T_f$  Versus Concentration for Different Materials

### 5.1 (b) Fourier Transform Spectroscopy

Although a Fourier Transform Spectrometer has been developed to measure absorptions in the wavelength range 0.1 mm to 3 mm this is still undergoing tests and as such is not yet fully operational. The measurements in this Section, therefore, refer to a sample whose wavelength dependent absorption was measured at the National Physics Laboratory, with the assistance of Dr James Birch.

The sample studied was a composite of aluminium particles dispersed in a decalin based  $\text{Fe}_3\text{O}_4$  ferrofluid ( $\bar{M}_G = 300\text{G}$ )

In Figure 19 the Fourier Transform Spectrum has been analysed to give the variation in the magnetic absorption with wavelength. Plotted on the y-axis is the ratio of the intensity through the sample with the field parallel to the plane of polarization of the incident radiation to the intensity through the sample with the field perpendicular to the plane of polarization (the latter being analogous to the quantity  $I_0$  defined in Section 4.3 (a)).

A magnetically induced absorption coefficient can also be calculated for the sample used in the FTS measurement. However, the normally defined coefficient of absorption takes into account the thickness of the sample and refers to a sample of fixed concentration. In this case the coefficient of absorption  $k'$  is given by

$$I = I_0 \exp(-k'x) \quad (24)$$

where  $I$  is the intensity of the radiation with the plane of polarisation parallel to the magnetic field and  $I_0$ , as stated previously, the intensity of the radiation with its plane of polarisation perpendicular to the field.  $x$  is the sample thickness.

For the sample used in this study  $x \approx 35 \mu\text{m}$ . From equation (24)

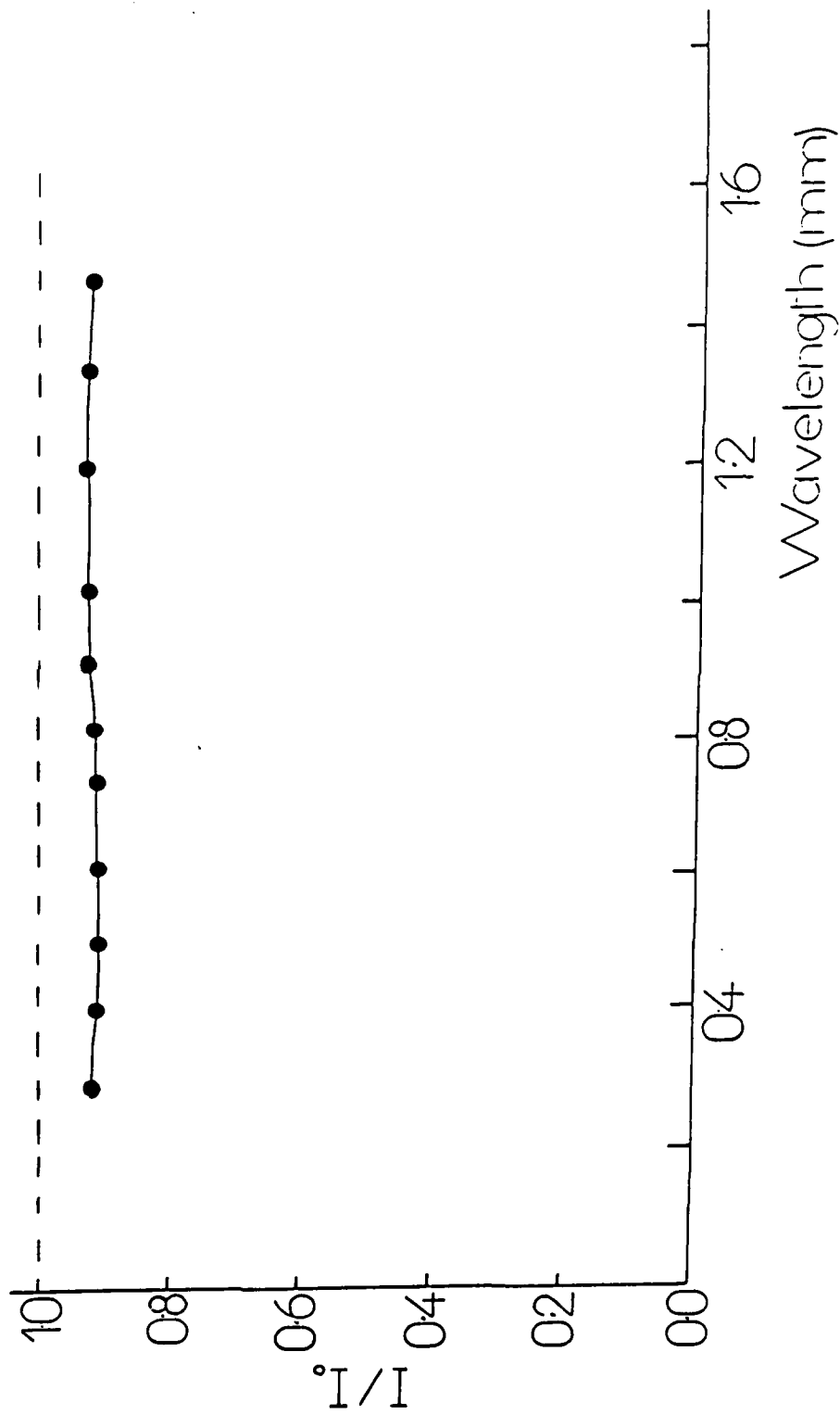


Figure 19 Plot of  $I/I_0$  Versus Wavelength for Aluminium Particles  
in Decalin Based Ferrofluid

$$\log_e(I/I_0) = -k'x \quad (25)$$

Since Figure 19 gives  $I/I_0 \approx 0.92$ ,  $k'$ (aluminium particles) =  $16.7 \text{ cm}^{-1}$

The absorption coefficient  $k'$  defined in this section and the absorption coefficient  $k$  defined in Section 5.1 (a) are related. Thus for a composite of thickness  $\Delta x$  and concentration  $c$

$$I = I_0 \exp(-kc) = I_0 \exp(-k'\Delta x) \quad (26)$$

$$\text{and } k' = \frac{kc}{\Delta x} \quad (27)$$

Taking a typical composite sample containing aluminium particles

$k = 6.11$  for  $c \approx 0.25$  and  $\Delta x = 0.1 \text{ cm}$ . Thus

$k'$  (Al particles)  $\approx 15 \text{ cm}^{-1}$ , which is the same order of magnitude as the value obtained from Fourier Transform Spectrometry. These measurements also indicate that  $k'$  should be constant over the wavelength range  $\lambda = 0.1$  to  $3 \text{ mm}$ .

It should be remembered that the sample is a monolayer and has a thickness of less than  $50 \mu\text{m}$ . The significant reduction in transmission ( $\approx 10\%$ ) through a single monolayer, indicating a relatively large magnetically induced absorption is encouraging in terms of possible applications in the near millimetre wavelength range.

#### 5.1 (c) Relaxation Measurements

Figure 20 shows a monolayer of  $10 \mu\text{m}$  diameter polystyrene spheres dispersed in a thin film of ferrofluid prepared as described in section 4.2. A magnetic field of  $\approx 100 \text{ Oe}$  has been applied to the sample in the plane of the film and the spheres have formed chains in the field direction.

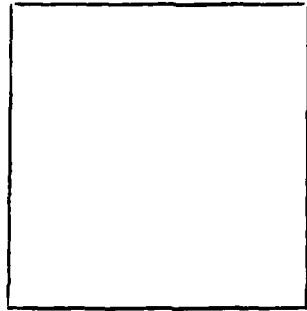


Figure 20 Composite Colloid Containing Polystyrene Spheres in a Field of 100 Oe Parallel to Layer

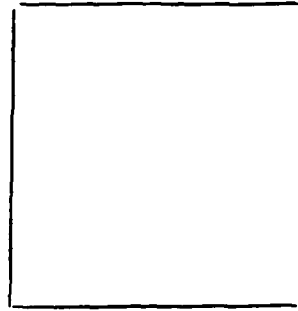


Figure 21 2-3 Seconds after Removal of Field

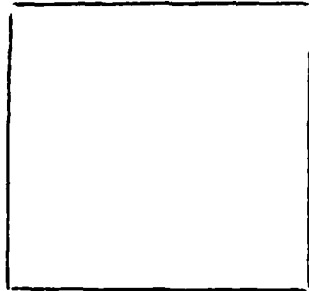


Figure 22 Composite Colloid Containing Tin Particles in a Field of About 100 Oe Parallel to Layer

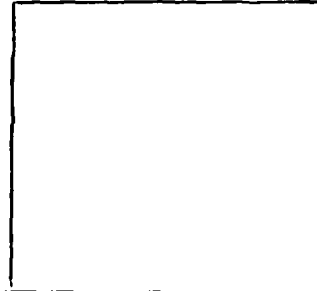
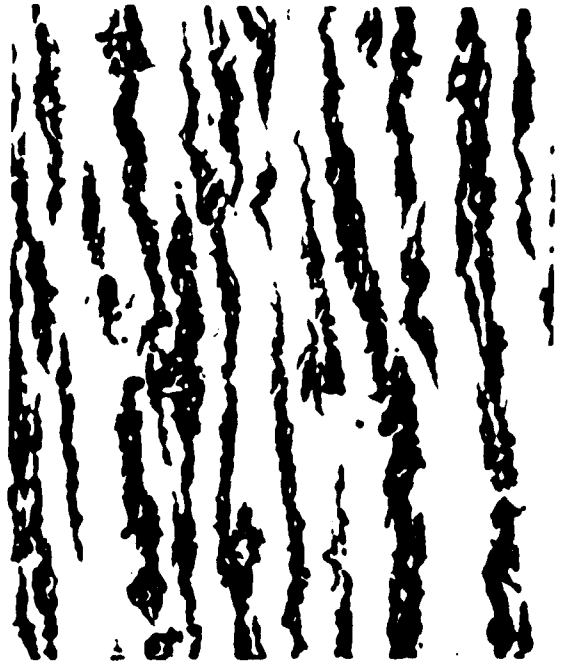
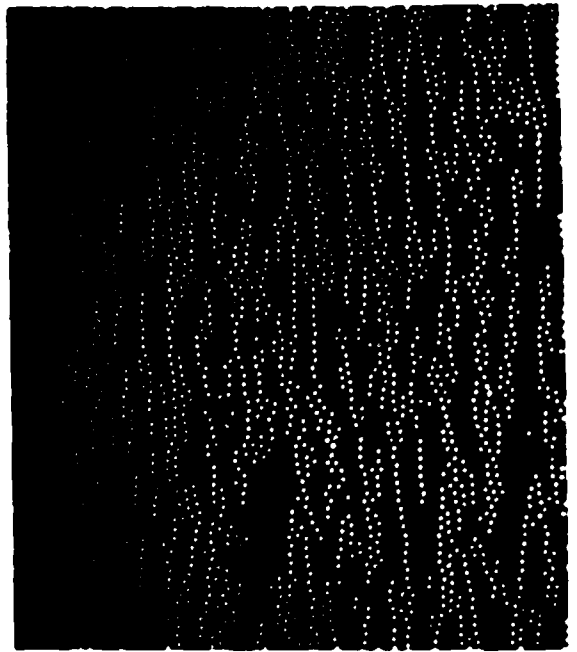
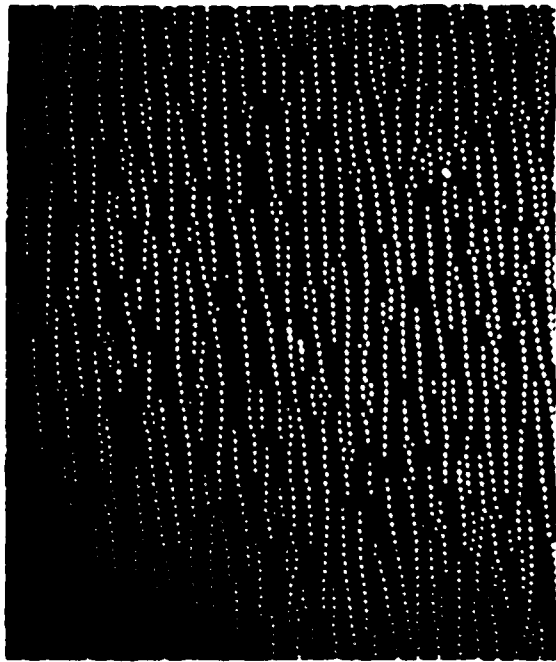


Figure 23 Composite Structure 2-3 Seconds after Removal of Field



When the field is removed, however, the chains kink and bend almost immediately to form the structure shown in Figure 21. Since diffusion of the relatively large polystyrene spheres is insignificant in a time scale of less than one second (Section 3.2) some other process must be responsible. The relaxation is probably due to surface tension effects once the field is removed. This would tend to draw the particles into a minimum energy configuration, i.e. a spherical cluster. This process is also evident in composites containing metallic particles dispersed in a ferrofluid. Figure 22 shows a sample of tin particles in a  $\text{Fe}_3\text{O}_4$  isopar M based ferrofluid ( $\bar{M}_S = 375\text{G}$ ). As in Figure 20 a magnetic field of about 100 Oe has been applied parallel to the layer of the film. The field was then removed and another photograph taken 2-3 seconds later. By this time the particles had formed the structure illustrated in Figure 23. The relaxation process is again unlikely to be due to a diffusion process and other factors such as the ferrofluid surface tension are more likely to be responsible.

Relaxation effects in composites containing metallic particles were also studied by monitoring the increase in the transmitted intensity  $I$  when the saturating field was removed from the sample (the experimental arrangement is that shown in Figure 11). Thus as the chains relax the alignment of the chains which was initially in the same direction as the plane of polarization of the incident radiation diminishes and the transmission thus increases.

Figure 24 shows the change in transmission as a function of time for two composites, one containing tin particles and a second containing copper particles in a ferrofluid ( $\bar{M}_S = 870\text{G}$ ).

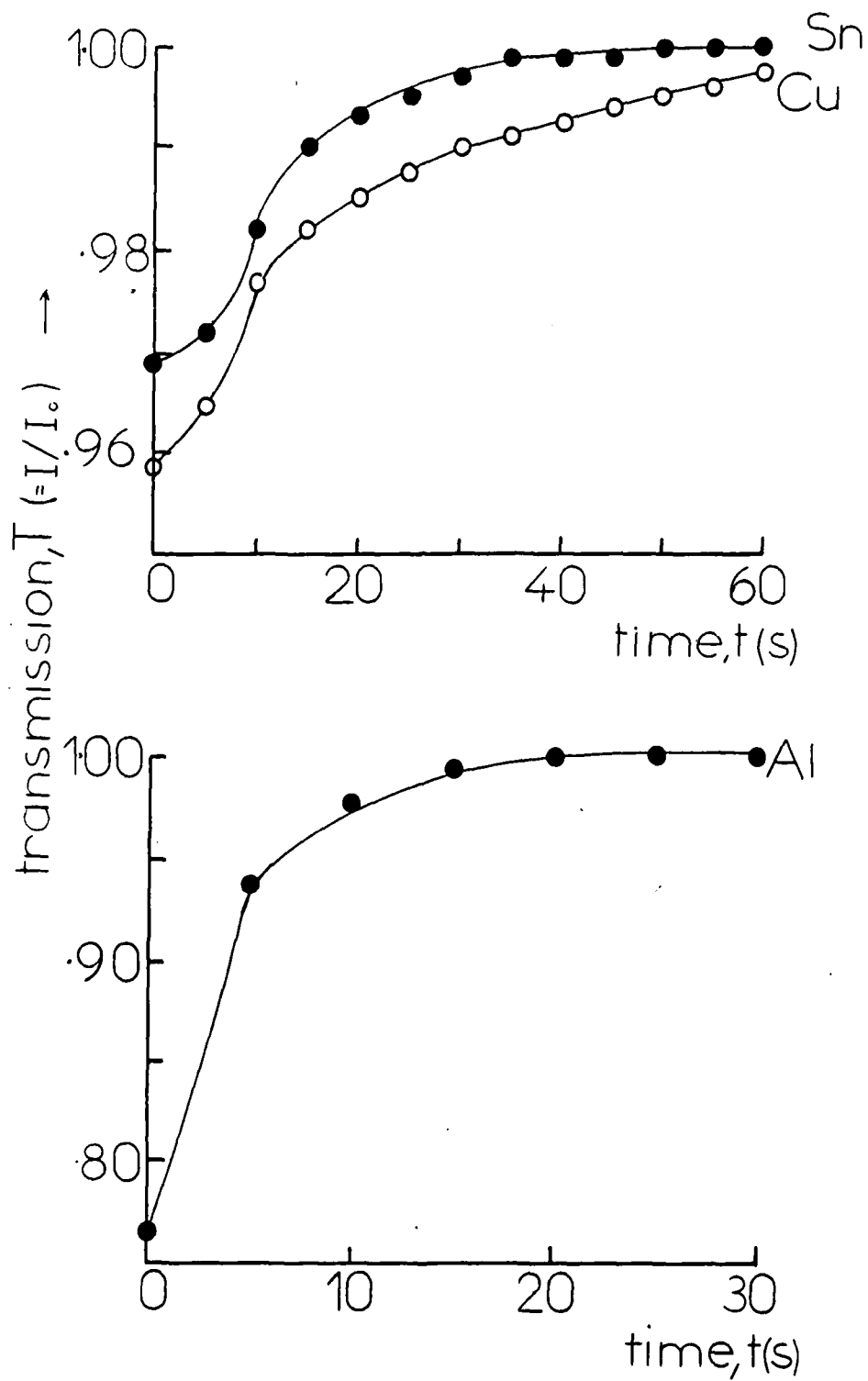


Figure 15 Relaxation of Aluminium Particles

It is again clear from Figure 24 that two relaxation mechanisms are operative. The initial relaxation takes place within seconds and over this time period the value of  $I$ , the transmitted intensity, increases rapidly. Following this initial relaxation a second slower relaxation process is evident and the rate of change of  $I$  with time decreases dramatically until equilibrium is reached and  $I$  then remains at a constant value.

The difference in the form of the curves in Figure 24 is probably due to a difference in the shape and size of the particles in the two samples.

Figure 25 shows the change in intensity  $I$  with time for a system of aluminium particles in a ferrofluid ( $\bar{M}_g = 375G$ ). As in Figure 24 two relaxation processes are again evident. The initial fast relaxation (0-10 seconds) is followed by a second slower relaxation taking several minutes. However, a significant difference between Figure 24 and Figure 25 is evident. The initial relaxation takes place more rapidly in the case of the aluminium particles in the 375 G ferrofluid than either tin or copper particles in the 870 G ferrofluid. This could be related to the different physical properties of the two carrier ferrofluids. For example both the viscosity and surface tension values would be different, the viscosity of the 870 G ferrofluid being much the greater because of higher particle concentration. The viscosity and surface tension of the ferrofluid carrier could therefore be an important consideration in the design of any device based on ferrofluid composites.

## 5.2 Monte-Carlo Simulations

### 5.2 (a) Theoretical configurations of a composite containing 1 $\mu\text{m}$ polystyrene spheres

Figure 26 shows the particle configuration predicted by the Monte-Carlo model for a composite containing 1000 polystyrene spheres ( $d = 1\mu\text{m}$ ) in a cell  $\approx 50 \mu\text{m}$  square. The resulting volume concentration is 0.16. The field applied parallel to the layer was 20 Oe and the ferrofluid has a susceptibility of  $\bar{\chi} = 0.05 \text{ emu/cc/Oe}$ . The corresponding experimental observation made using optical microscopy on a sample under similar conditions is shown in Figure 27.

Figure 28 shows the configuration generated for a more dilute system of 400 particles in the same size cell and under the same conditions of field and susceptibility. This number of particles corresponds to a volume concentration  $c$  of 0.06. Figure 30 shows the experimental observation for a sample under similar conditions as Figure 28.

Figure 31 shows the structure predicted by the model for a sample with a volume concentration  $c$  of 0.16 with a field of 110 Oe applied perpendicular to the plane of the composite. This produces a triangular or hexagonal lattice formed by repulsive magnetic dipoles, the experimental result of which is shown in Figure 32.

### 5.2 (b) Spatial Distribution Function $g(r, \theta)$

The spatial distribution function  $g(r, \theta)$  calculated from the Monte-Carlo configuration gives a quantitative measure of the spatial texture induced by the magnetic field. Figure 33 shows  $g(r, \theta)$  for the 1000 sphere Monte-Carlo simulation shown in Figure 26 with a field of 20 Oe applied parallel to the plane of the film.

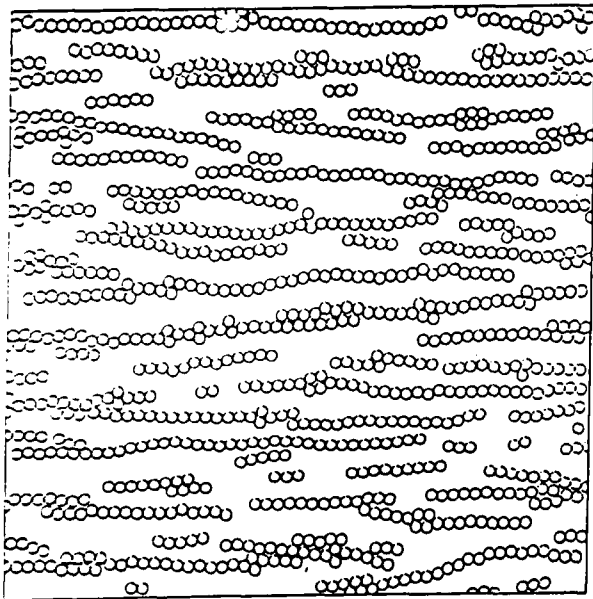


Figure 26 Monte-Carlo Configuration with  
H Parallel to Film,  $C = 0.16$

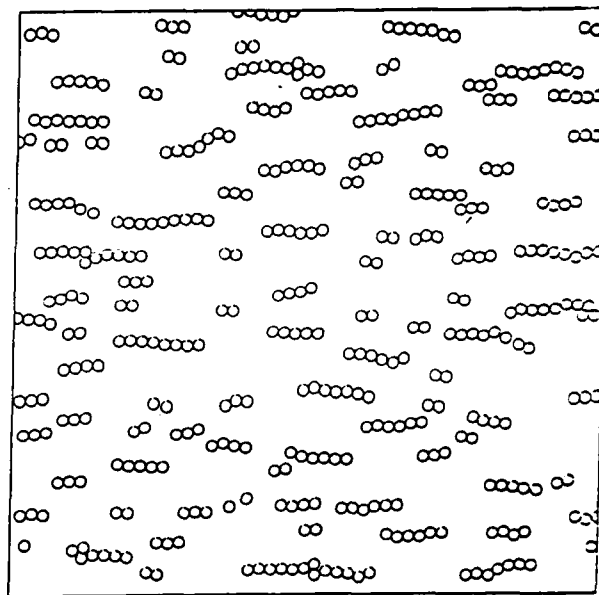


Figure 27 Monte-Carlo Configuration  
with H Parallel to Film,  
 $C = 0.06$

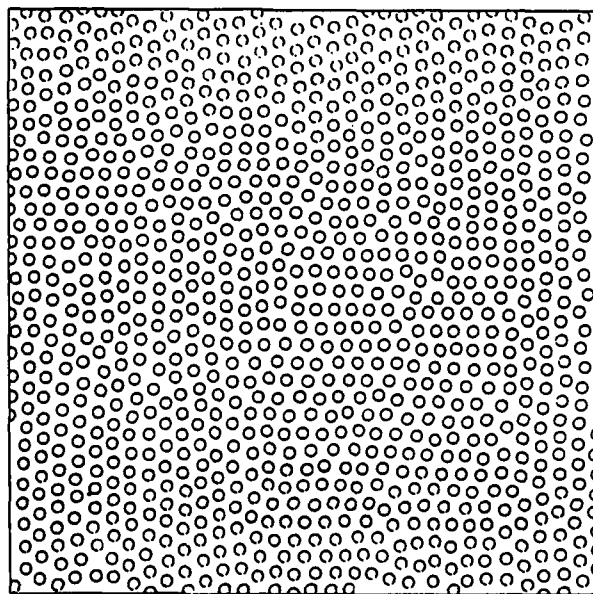


Figure 28 Monte-Carlo Configuration with H Perpendicular to Film,  $C = 0.16$

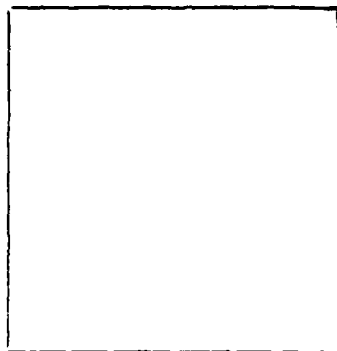


Figure 29 Composite Colloid Containing Polystyrene Spheres in Field of 20 Oe Applied Parallel to the Film,  $C = 0.16$

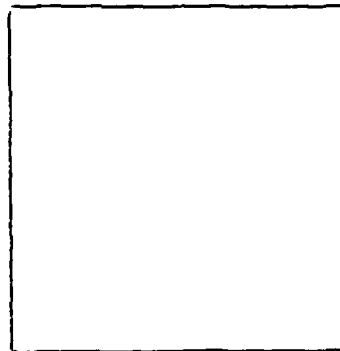


Figure 30 Composite Colloid Containing Polystyrene Spheres in a Field of 20 Oe Applied Parallel to the Film,  $C = 0.06$

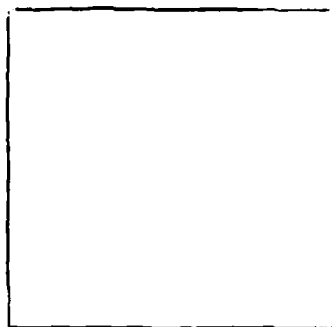
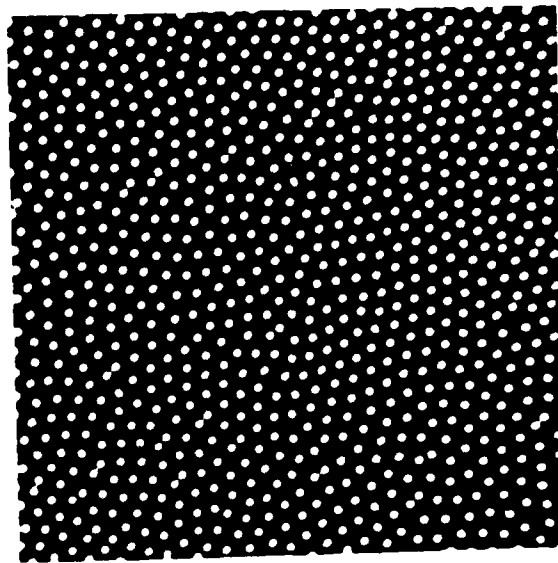
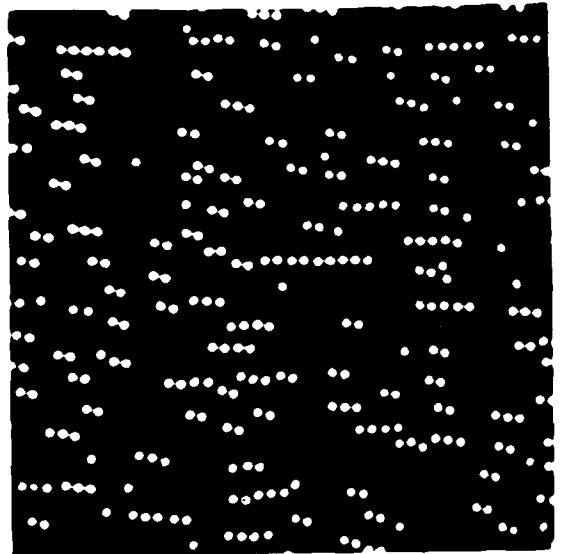
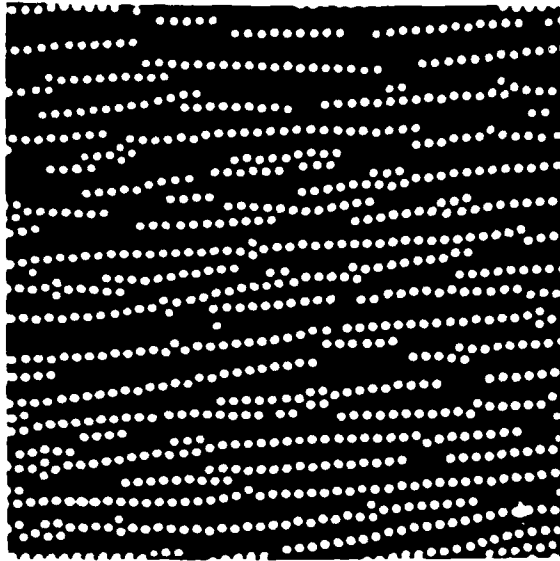


Figure 31 Composite Colloid Containing Polystyrene Spheres in a Field of 20 Oe Applied Perpendicularly to the Film,  $C = 0.16$



The value of  $\theta$  in this case is 0, i.e.  $g(r, \theta)$  is measured in the field direction. It can be seen that peaks occur in  $g(r, 0)$  at integer values of particle diameter indicating that chains of touching particles have formed. Peak structure can be seen up to 18 particle diameters and Figure 33 is thus the 'signature' of a strongly interacting system of particles.

Figure 34 shows  $g(r, 0)$  for the 400 particle case, i.e.  $c = 0.06$  corresponding to the structure shown in Figure 28. It is similar to Figure 33 in that the peaks, which again occur at integer diameter values are sharp and well defined indicating touching spheres. However, the average chain length in the less dense system is lower, as would be expected, and this is shown by the extent of the peak structure in the function  $g(r, 0)$ . Structure persists only as far as 5-6 particle diameters in this case. Figure 34 is therefore the 'signature' for a low concentration, strongly interacting system of particles.

Figure 35 shows  $g(r, 0)$  for the triangular lattice shown in Figure 31 where the field is perpendicular to the sample plane. Sharp peaks are still evident, indicating a regular structure. However, in this case the peak spacing gives the average particle separation which may be described as a pseudo lattice parameter.

#### 5.2 (c) Energy Considerations

Monte-Carlo techniques have been used to evaluate the internal energy (in reduced units,  $U/kT$ ) of the composite as a function of the angle between the applied magnetic field and the plane of the film,  $\phi$ . The energy predicted is shown in Figure 36. This shows that the high energy of the composite arising from particle repulsions when the field is perpendicular to the plane of

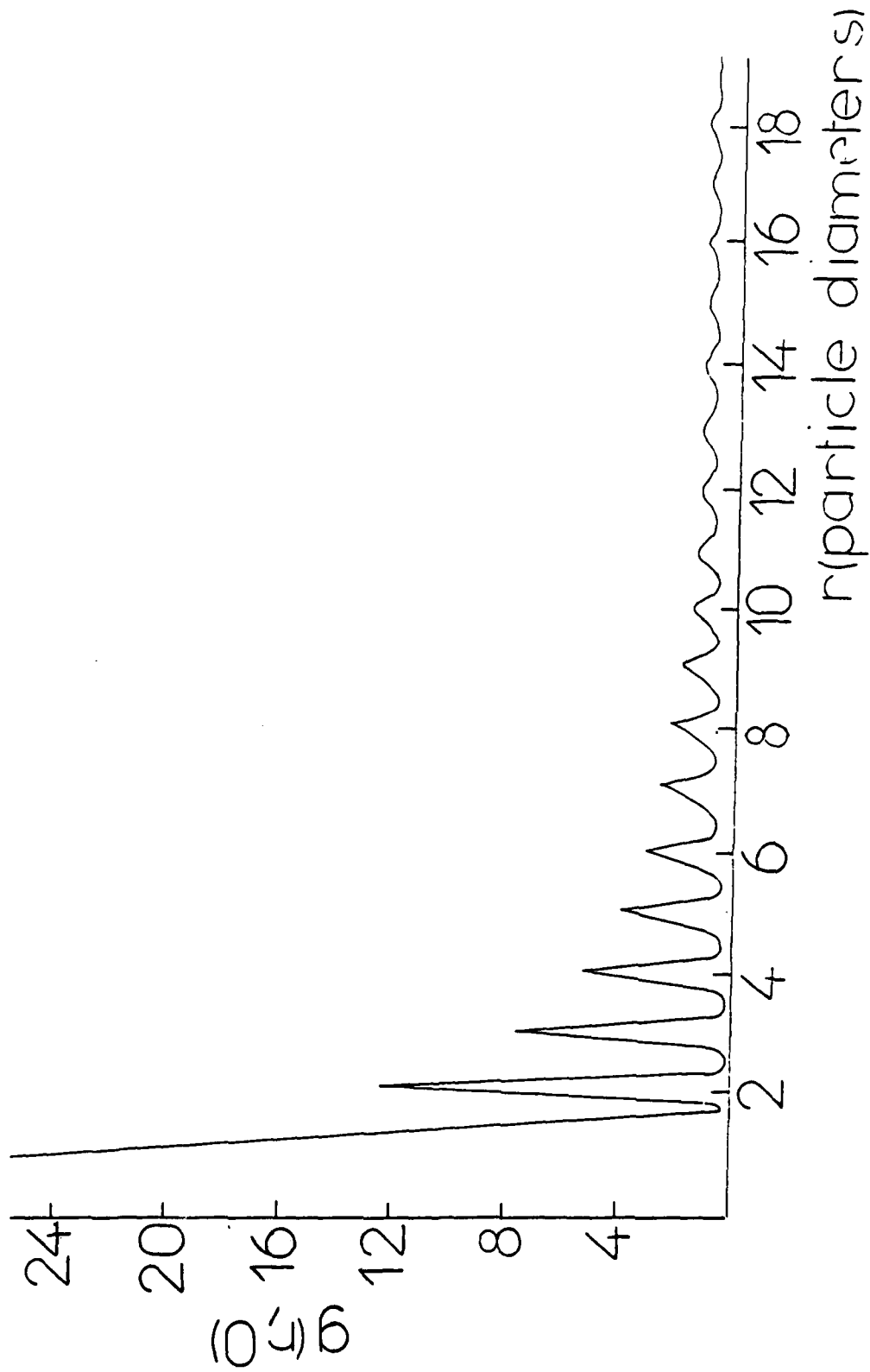


Figure 32 The Spatial Distribution Function of Figure 26

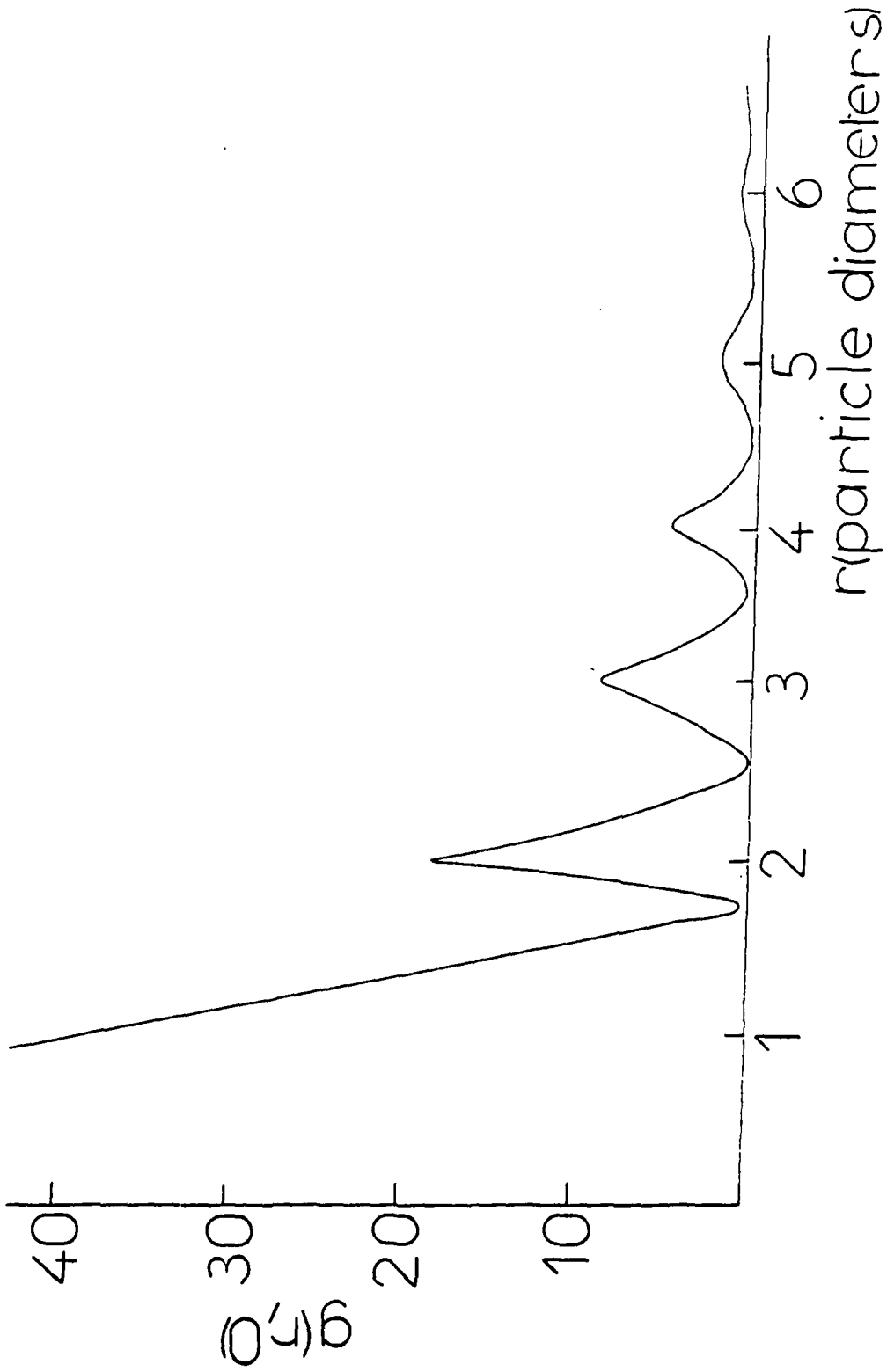


Figure 33 The SDF of Figure 27

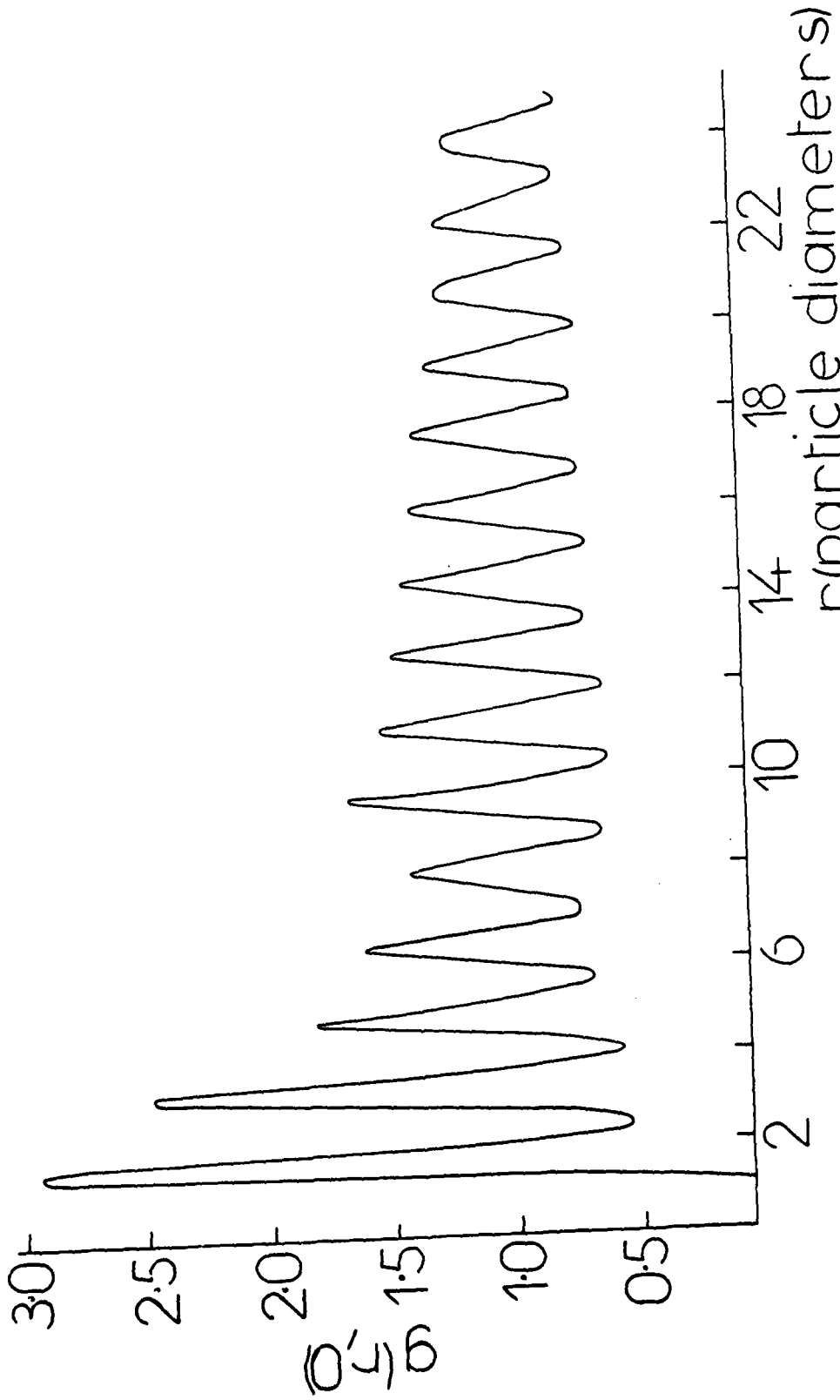


Figure 34 The SDF of Figure 28

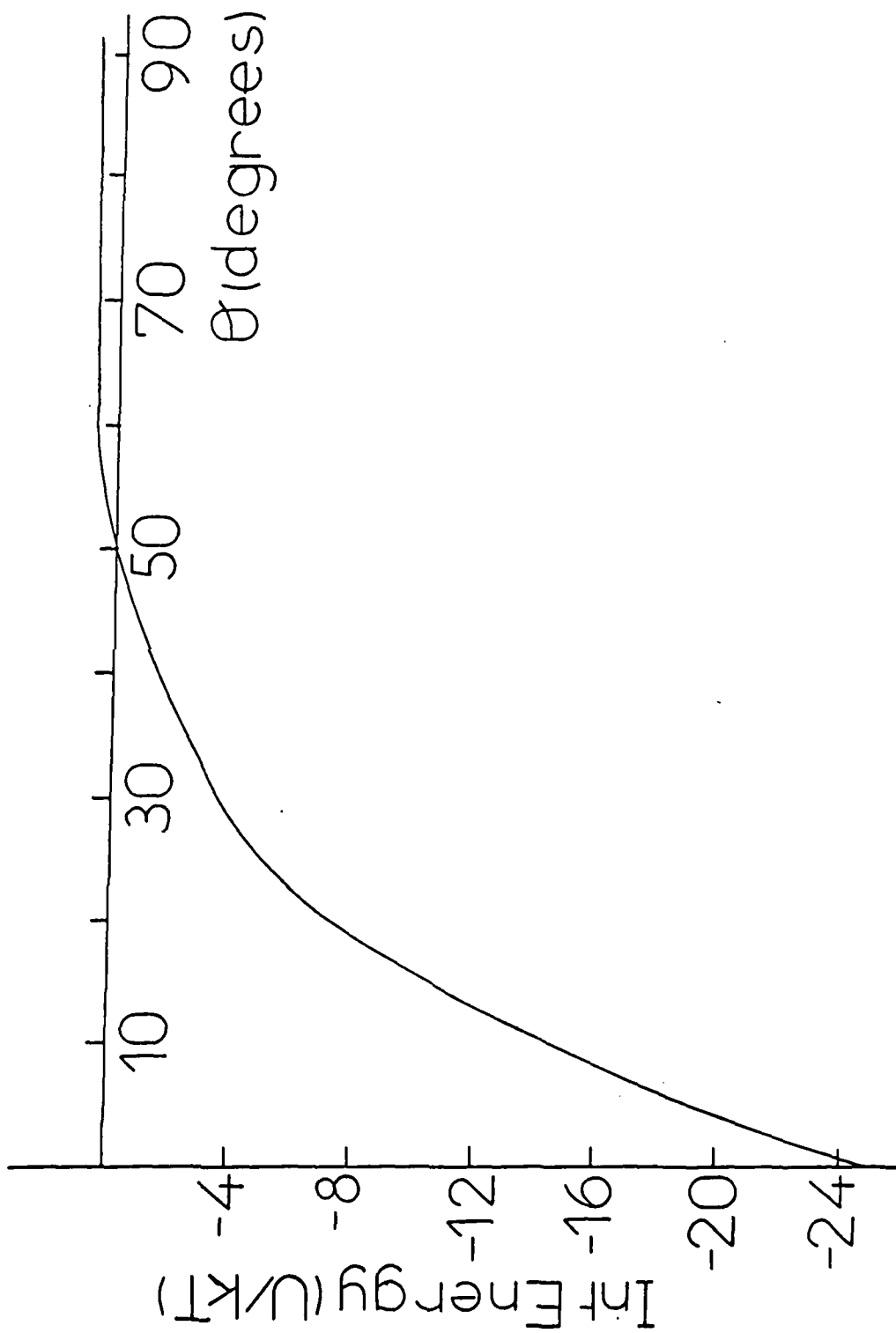


Figure 35 Internal Energy of a Composite Colloid Plotted as a Function of the Angle between the Field and the Plane of the Film

the film is reduced progressively as the field direction is changed and is lowest when the field is parallel to the plane of the film. A change in composite structure from the triangular lattice to a system of parallel chains has been predicted to take place at  $\phi = 60^\circ$ , which can be compared with the value of  $\approx 70^\circ$  proposed by Skjeltorp (1984).

6      Recommendations and Future Work

The absorption of millimetre microwave radiation by ferrofluid composites in the form of a thin film subjected to a magnetic field (magnetic dichroism) is remarkable in that a monolayer of <50 microns in thickness is capable of absorbing a significant amount of radiation, the amount depending on the particle concentration, the particle materials and the applied magnetic field. Very large, 60% absorptions, can be readily achieved in thicker samples in magnetic fields of less than 100 Oersteds. What is also significant is that improved sample preparations arising from further studies are likely to give even greater absorptions. At this stage of the investigation the effects of particle size and carrier fluid magnetisation on the magnetic dichroism remain uncertain. However, it is confidently expected that substantial improvements can be made. There are potentially many exciting applications of ferrofluid composites in the near millimetre wavelength range based on magnetically induced absorptions which are worthy of exploitation.

The studies to date have been mainly concerned with establishing real effects and noting their magnitudes. Measurements during the coming year will concentrate more on obtaining quantitative measurements and details of the frequency dependence of the magnetic dichroism and birefringence. This will be completed by the end of the Project. A Microwave Fourier Transform Spectrometer has been constructed to assist in this investigation.

A more detailed study will require measuring the effect of magnetic fields and the effect of the composite particle size and concentration. As has been shown it is possible to model the structure of the composites using Monte-Carlo calculations and theoretical predictions of experiments observations are, therefore, possible.

A final study will include the production of a composite with properties which maximise the already large absorptions in the near millimetre microwave range.

The study of the microwave properties of ferrofluid composites has proved rewarding and valuable. There are many variables, however, which are likely to affect performance. Not all of these can be studied before the conclusion of the present project. In particular the effect of the carrier fluid, its magnetic properties and viscosity can only be studied briefly in the time available. Relaxation effects relating to the diffusion of particles when the applied magnetic field is removed have to be studied if devices using composites are to be developed. A guide to what can be realistically completed by the end of the final year of the contract is given at the end of this Section together with a proposal for further work as an extension to the current project.

Finally, it is the anisotropies induced in the composites by a magnetic field that are responsible for the observed microwave properties. The anisotropies, however, can also lead to interesting optical, electrical, dielectric and rheological properties. Studies of these are important and complement current microwave studies. The immediate concern, however, is to produce reliable, stable composite systems which show striking effects in the near millimetre wavelength range. The construction of simple devices then becomes worthwhile.

During 1985/86 the following programme of work will be undertaken as a priority.

- (1) A study of the wavelength dependences of the magnetic dichroism and birefringence.

(2) A theoretical study of composite structures using Monte-Carlo calculations with a view to establishing optimum conditions for absorption in the microwave region

(3) Absolute measurements of absorption in terms of particle size and concentration.

(4) A preliminary study of devices using magnetic fluid composites.

Further measurements may be possible but the following would be a valuable programme of study for an extension to the current project.

(5) A study of the effects of particle shape, chain length and carrier fluid on the magnetic dichroism in the microwave region.

(6) Measurement of relaxation effects in composites and techniques for shortening relaxation times by applying secondary fields to break up chain formation.

(7) A study of the stability of composites in gravitational and magnetic field gradients as a precursor to device development.

(8) The preparation of new composite materials containing optically active particles and others containing strongly magnetic particles.

(9) An examination of the properties of composites containing sub-micron particles, approaching molecular sizes. Such materials become equivalent to 'alloys' and the alignment of the 'molecular' particles could be studied in an external magnetic field. If the particle sizes in the composite can be reduced to molecular sizes then composite Langmuir-Blodgett type thin films become possible. This would be of interest in the rapidly developing field of molecular electronics.

As much of the above programme as possible will be undertaken before the contract terminates in September 1986. It is hoped, however, that it will be able to continue the work beyond this period.

Acknowledgements

The Authors would like to acknowledge contributions made to this research project by Drs A Bradbury, K O'Grady, R W Chantrell and Mr G Martin. Special thanks are due to Dr J Birch of the National Physical Laboratory for his continued and untiring support in helping to develop the Fourier Transform Spectrometer.

Mr S Wells (UCNW) is also thanked for helping to prepare samples and Mrs M C Jones for typing this Report.

REFERENCES

- 1 Birch, J.R., Bentley, C.A. and Llewellyn, J.P., *Electronics Letters*, Vol. 21, No. 8, 11 April (1985).
- 2 Popplewell, J., Davies, P., Llewellyn, J. and O'Grady, K., *J. Mag. Magn. Mat.* (to be published (1985)).
- 3 Hartman, U. and Mende, H.H., *J. Mag. Magn. Mats.*, 45, 409 (1984).
- 4 Davies, H.W. and Llewellyn, J.P., *J. Phys. D: Appl. Phys.*, 12, (1979).
- 5 Bogardus, H., Krueger, D.A. and Thompson, D., *J. Appl. Phys.*, 49, 6, 3422, (1978).
- 6 Wiener, O., *Abstracts Akad. Wiss*, 32, 509 (1912).
- 7 Bragg, W.L. and Pippard, A.B., *Acta. Cryst.* 6, 685 (1953).
- 8 Llewellyn, J.P., *J. Phys. D. Appl. Phys.* 16 pp 95-104, (1983).
- 9 Chantrell, R.W., Bradbury, A. and Meneer, S., *J. Appl. Phys.*, 57, 4268 (1985).
- 10 Skjelthorp, A.T., *Phys. Rev. Letts.*, 51, No. 25, (1983).
- 11 Davies, P., Popplewell, J., Martin, G.A.R., Bradbury, A. and Chantrell, R.W., *J. Phys. D.* (to be published 1986)

- 12 Shimoiisaka, K., Vokoyama, H. and Nakatsuka, J. Jpn Soc., Powder Metall., 28, 210, (1980).
- 13 Chantry, G.W., Evans, M.H., Chamberlain, J., and Gebbie, H.A., Infrared Physics, 9, 31-31, (1969).
- 14 Golay, M.J.E., Rev. Sci. Inst., 18, No. 5, (1947).
- 15 Golay, M.J.E., Rev. Sci. Inst., 20, No. 11, (1949).
- 16 Rollin, B.V., Proc. Phys. Soc., 77, 1102, (1961).
- 17 Rollin, B.V. and Kinch, M.A., Br. J. Appl. Phys., 14, pp 672-676, (1963).
- 18 Jefferies, R., Birch, J.R., Hawker, B. and Atkins, A., Infrared Phys., 24, No. 2/3, pp 333-338, (1984).
- 19 Menear, S., Bradbury, A. and Chantrell, R.W., J. Mag. Mag. Mat., 43, 166, (1984).
- 20 Menear, S., Thesis, University of Wales, (1984).
- 21 O'Grady, K., Popplewell, J. and Charles, S.W., J. Mag. Mag. Mat., 39, 86, (1983).

22 Meneer, S., Bradbury, A. and Chantrell, R.W., Proc. I.C.M.,  
San Francisco, (to be published 1966).

23 Chantrell, R.W., Bradbury, A., Popplewell, J. and Charles, S.W.,  
J. Phys. D. Appl. Phys., 13, L119, (1980).

Publications Arising 1985

- 1 Magnetic and Optical Properties of Magnetic Fluids,  
J. Popplewell and J.P. Llewellyn, Proc. of Int. Symp. on the Physics of  
Complex and Supermolecules. Pub. John Wiley (1985).
- 2 Diffraction Effects in Magnetic Fluid Composites,  
P. Davies, J. Popplewell, J.P. Llewellyn and K. O'Grady, J. Phys. C:  
Solid State Phys., 18, L661 (1985).
- 3 Monte-Carlo Simulations of the Structure of Magnetic Fluid Composites,  
P. Davies, J. Popplewell, G. Martin, A. Bradbury and R.W. Chantrell,  
J. Phys. D., Accepted for Publication (1985).
- 4 Microwave Properties of Ferrofluid Composites,  
J. Popplewell, P. Davies, J.P. Llewellyn and K. O'Grady, Proc. of Int.  
Conf. on Magnetism, San Francisco. J. Mag. Mag. Mats. (To be published  
1985).
- 5 Microwave Absorption in Ferrofluid Composites Containing Metallic  
Particles,  
J. Popplewell, P. Davies and J.P. Llewellyn, Int. Conf. on Magnetic  
Fluids, Tokyo. (To be published 1986).
- 6 Chain Formation in Ferrofluid Composites,  
P. Davies, J. Popplewell, G. Martin, A. Bradbury and R.W. Chantrell,  
Int. Proc. of Intermag 1986. (To be published 1986).

END

DATE  
FILMED

2-86

DTI